Supporting Information

Charge-regulated hepatic *γ*-glutamyltranspeptidase fluorescent probe: *in vivo* staging *Schistosoma*-infection

Xiaoxi Ma[a], Eryang Xie[a], Qiang Li[c], Chuyang Sun[a], Yongkang Yao[a], Chenxu Yan*[,a], Qianfu Luo*[,a], Zhiqian Guo*[,a,b] & Wei-Hong Zhu[a]

[a]*Key Laboratory for Advanced Materials and Institute of Fine Chemicals, Feringa Nobel Prize Scientist Joint Research Center, Frontiers Science Center for Materiobiology and Dynamic Chemistry, School of Chemistry and Molecular Engineering, East China University of Science and Technology, Shanghai 200237, China. E-mail: chenxuyan@ecust.edu.cn; luoqf@ecust.edu.cn; guozq@ecust.edu.cn.*

[b]*State Key Laboratory of Bioreactor Engineering, East China University of Science and Technology, Shanghai 200237, China.*

[c]*National Key Laboratory of Intelligent Tracking and Forecasting for Infectious Diseases, National Institute of Parasitic Diseases at Chinese Center for Disease Control and Prevention, Chinese Center for Tropical Diseases Research, National Research Center for Tropical Diseases, Key Laboratory of Parasite and Vector Biology, National Health Commission, WHO Collaborating Center for Tropical Diseases, National Center for International Research on Tropical Diseases, Ministry of Science and Technology, Shanghai 20025, China.*

Contents

1. Experiment section

Materials and general methods

Unless specially stated, all solvents and chemicals were purchased from commercial suppliers in analytical grade and used without further purification. Tetrahydrofuran (THF), petroleum ether (PE), ethyl acetate (EA), dichloromethane (DCM), dimethyl sulfoxide (DMSO), methanol (MeOH) and acetonitrile (MeCN) were obtained from General-Reagent (Shanghai, China). Hoechest 33342 was purchased from Beyotime Biotechnology (Shanghai); The ^{1}H and ^{13}C NMR spectra were recorded on a Bruker AM 400 spectrometer, using TMS as an internal standard. High resolution mass spectrometry data were obtained with a Q Exactive™ UHMR spectrometer (Thermo Fisher Scientific). Absorption spectra were collected on a Varian Cary 500 spectrophotometer, and fluorescence spectra measurements were performed on a Varian Cary Eclipse fluorescence spectrophotometer. Confocal fluorescence images were taken on a confocal laser scanning microscope (CLSM, Leica confocal microscope STELLARIS 8 FALCON). In vivo fluorescence images were measured with a PerkinElmer IVIS Lumina Kinetic Series III imaging system.

Synthesis of QMC-C-GGT, QMC-SO_3-GGT and QMC-N-GGT

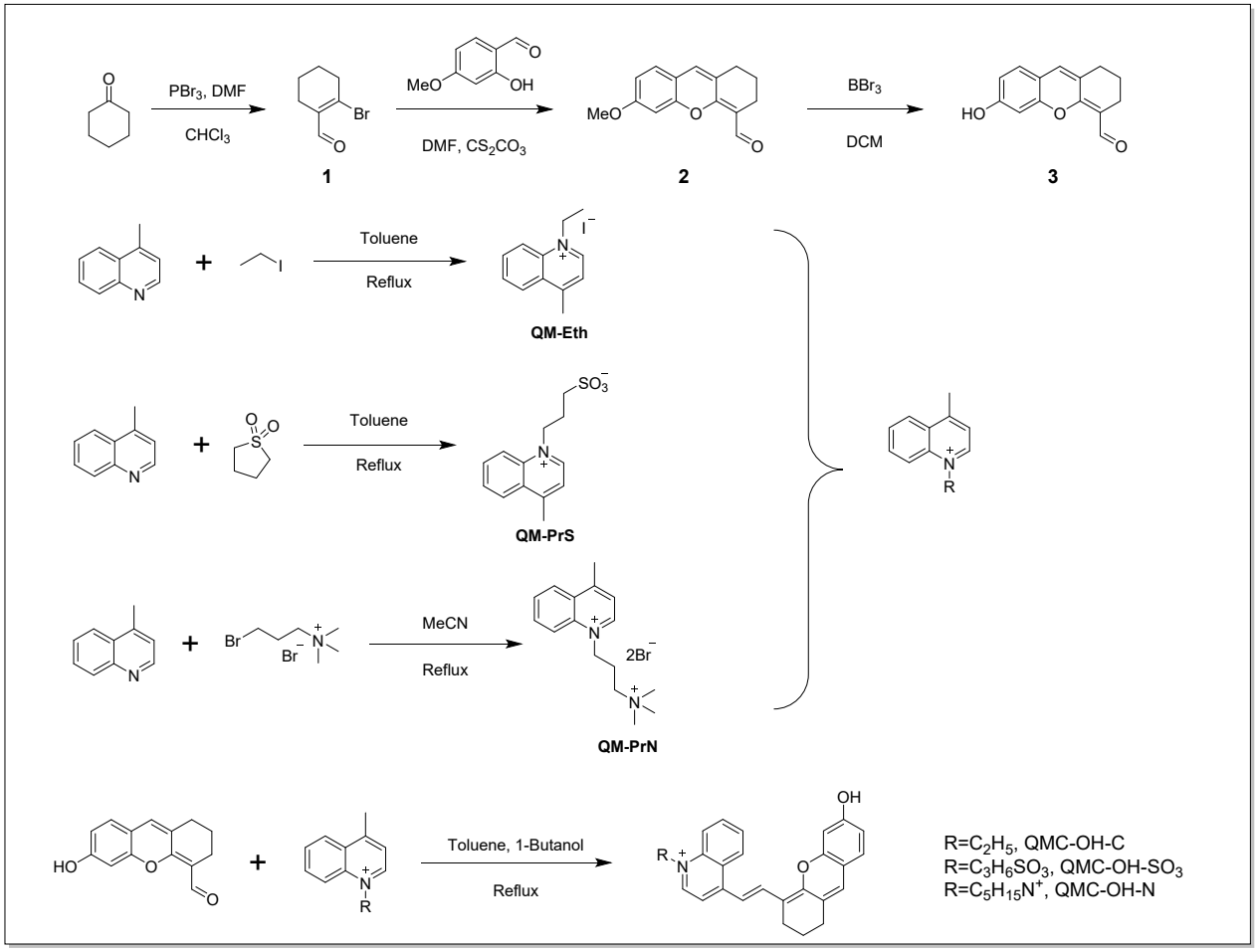

Scheme S1 Synthetic route of QMC-OH-C, QMC-OH-SO_3 and QMC-OH-N

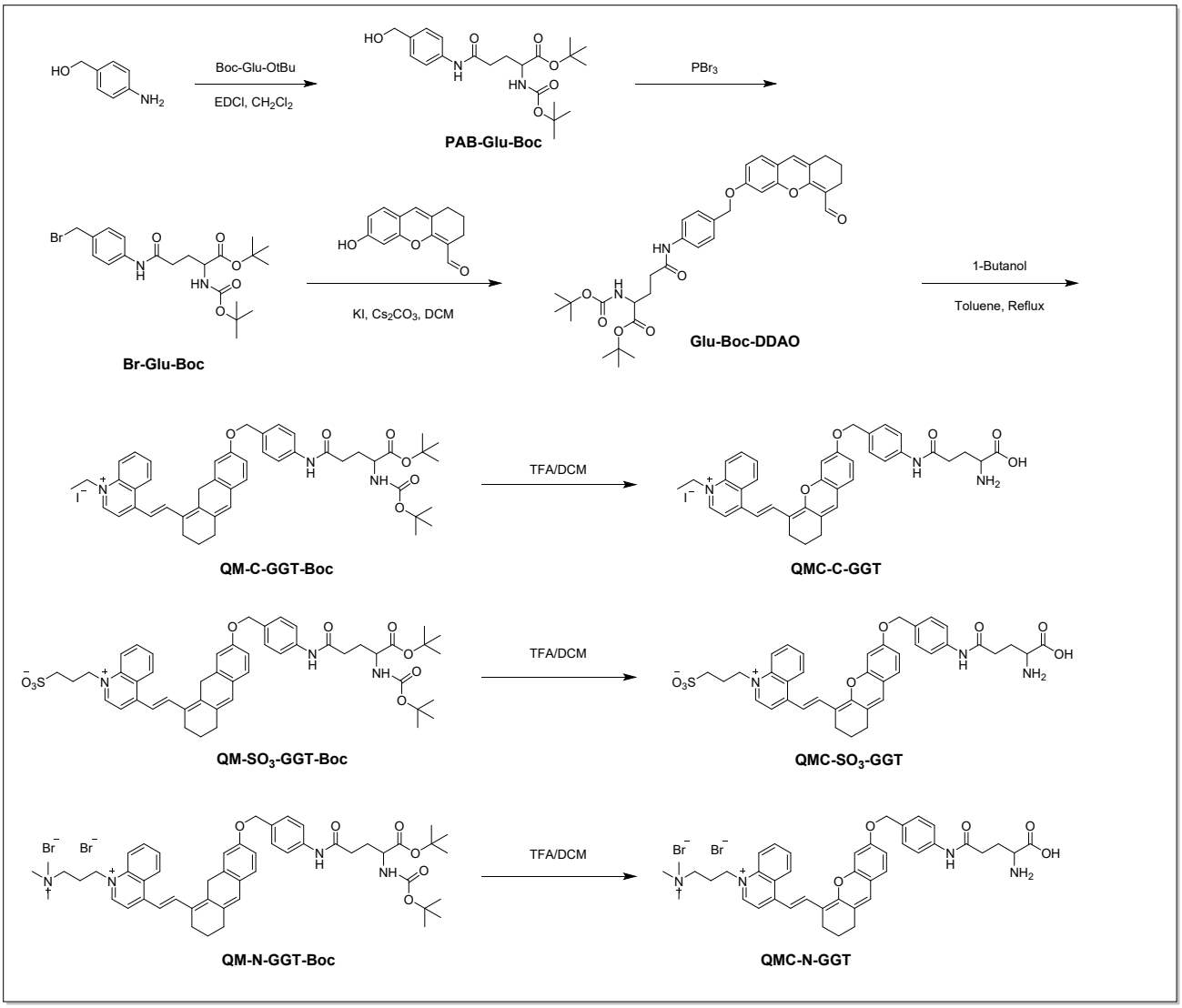

Scheme S2 Synthetic route of QMC-C-GGT, QMC-SO_3-GGT and QMC-N-GGT

Synthesis of QM-Eth

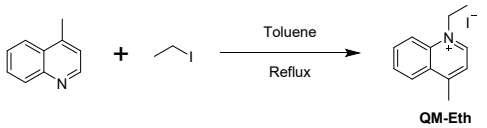

4-methylquinoline (3.0 g, 28.0 mmol) and Iodoethane (5.61 g, 36.0 mmol) were dissolved in toluene (10 mL). Then the mixture was stirred for 6 h at 120 °C under an argon atmosphere. The product was filtered off purified by washed with acetonitrile to obtain a yellow solid (6.7 g): Yield 80%.^{1}H NMR (400 MHz, DMSO-d_6, ppm): δ 1.60 (t, J = 7.2 Hz, 3H, -CH_3), 3.02 (s, 3H,-CH_3), 5.07 (q, J = 7.0 Hz, 2H, -CH2-), 8.07 (t, J = 7.4 Hz, ^{1}H, Ph-H), 8.10 (d, J = 6.2 Hz, 1H, Ph-H), 8.28 (t, J = 7.9 Hz, 1H, Ph-H), 8.56 (d, J = 8.4 Hz, 1H, Ph-H), 8.62 (d, J = 8.9 Hz, 1H, Ph-H), 9.45 (d, J = 6.0 Hz, 1H, Ph-H). ^{13}C NMR (100 MHz, DMSO-d_6, ppm): δ 15.24, 19.75, 52.51, 119.23, 122.77, 127.17, 128.86, 129.54, 135.08, 136.49, 148.09, 158.31.

Synthesis of QM-PrS

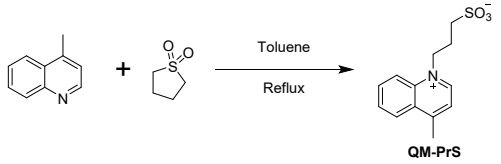

4-methylquinoline (4.9 g, 33.3 mmol) and 1,3-Propanesultone (4.1 g, 33.3 mmol) were dissolved in toluene (20 mL). Then the mixture was stirred for 8 h at 120 °C under an argon atmosphere. After reaction, the mixture was filtered under suction, washed with ethanol and then vacuum-dried to obtain the white product (6.2 g): Yield 56%. ^{1}H NMR (400 MHz, MeOD, ppm): δ 2.48-2.52 (m, 2H, -CH_2-), 2.98 (t, J = 6.6 Hz, 2H, CH_2-), 3.06 (s, 3H, -CH_3), 5.24 (t, J = 7.8 Hz, 2H, -CH_2-), 7.96 (d, J = 6.1 Hz, 1H, Ph-H), 8.04 (t, J = 7.7 Hz, 1H, Ph-H), 8.27 (t, J = 7.7 Hz, 1H, Ph-H), , 8.56 (d, J = 8.4 Hz, 1H, Ph-H), 8.66 (d, J = 8.8 Hz, 1H, Ph-H), 9.27 (d, J = 5.8 Hz, 1H, Ph-H). ^{13}C NMR (100 MHz, MeOD, ppm): δ 20.27, 26.89, 57.36, 120.32, 123.88, 128.29, 131.08, 136.81, 149.42, 161.03.

Synthesis of QM-PrN

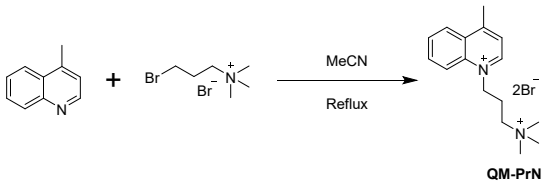

4-methylquinoline (200 mg, 1.4 mmol) and (3-Bromopropyl) trimethylammonium bromide (365 mg, 1.4 mmol) were dissolved in toluene (10 mL). Then the mixture was stirred for 24 h at room temperature under an argon atmosphere. The solvent was removed under reduced pressure. The crude product was dissolved in acetonitrile and then added dropwise into ethyl acetate. Gray solid product formed in the solution (366 mg): Yield 58%. ^{1}H NMR (400 MHz, MeOD, ppm): δ 2,90 (d, J = 5.2 Hz, 2H, -CH_2-), 3.48 (s, 9H, C(CH_3)$_3$), 4.06 (t, J = 8.0 Hz, 2H, -CH_2-), 5.43 (t, J = 7.6 Hz, 2H, -CH_2-), 8.23-8.32 (m, 2H, Ph-H), 8.54 (t, J = 8.0 Hz, 1H, Ph-H), 8.82 (d, J = 8.4 Hz, 1H, Ph-H), 8.99 (d, J = 8.8 Hz, 1H, Ph-H), 9.70 (d, J = 5.6 Hz, 1H, Ph-H). ^{13}C NMR (100 MHz, MeOD, ppm): δ 20.57, 25.10, 54.15, 55.11, 64.00, 120.44, 123.20, 128.51, 131.18, 137.13, 138.82, 138.82, 149.60, 161.59. HRMS (ESI-MS) m/z: calcd

for $[C_{16}H_{24}N_2]^{2+}$: 122.0964, found: 122.0966.

Synthesis of QMC-OH-C

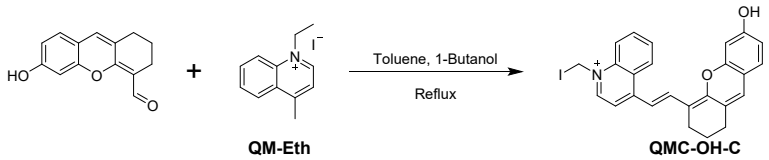

QM-Eth QMC-OH-C

Compound 3 (50 mg, 0.22 mmol) and QM-Eth (98 mg, 0.33 mmol) were dissolved in toluene (8 mL) and 1-butanol (4 mL). Then the mixture was stirred for 10 h at 110 °C under an argon atmosphere. After reaction, the mixture was filtered under suction, washed with ethanol and then vacuum-dried to obtain the black product (50 mg): Yield 60%. ^{1}H NMR (400 MHz, DMSO-d_6, ppm): δ 1.55 (t, J = 6.8 Hz, 3H, -CH_3), 1.80 (s, 2H, -CH_2-), 2.60 (s, 2H, -CH_2-), 2.72 (s, 2H, -CH2-), 4.88 (t, J = 8.0 Hz, 2H, -CH_2-), 6.63 (d, J = 8.4 Hz, 1H, Ph-H), 6.84 (s, 1H, Ph-H), 6.92 (s, 1H, Ph-H), 7.19 (d, J = 8.0 Hz, 1H, Ph-H), 7.35 (d, J = 15.2 Hz, 1H, alkene-H), 7.90 (t, J = 7.6 Hz, 1H, Ph-H), 8.28 (d, J = 6.8 Hz, 1H, Ph-H), 8.38 (d, J = 8.9 Hz, 2H, Ph-H), 8.49 (d, J = 15.1 Hz, 1H, alkene-H), 8.85 (d, J = 8.8 Hz, 1.3 Hz, 1H, Ph-H), 9.01 (d, J = 6.7 Hz, 1H, Ph-H), 10.26 (s, 1H, -OH). ^{13}C NMR (100 MHz, DMSO-d_6, ppm): δ 15.04, 20.35, 24 .25, 28.74, 51.06, 102.18, 112.07, 112.11, 113.64, 114.13, 118.62, 125.86, 125.99, 126.30, 127.03, 127.84, 128.26, 134.46, 137.60, 137.66, 145.30, 152.38, 153.69, 154.44, 159.79. HRMS (ESI-MS) m/z: calcd for $[C_{26}H_{24}NO_2]^+$: 382.1802, found: 382.1797.

Synthesis of QMC-OH-SO_3

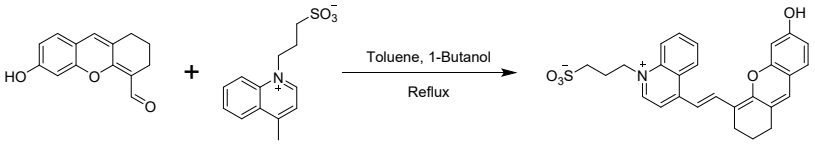

QM-PrS QMC-OH-SO_3

Compound 3 (50 mg, 0.22 mmol) and QM-PrS (116 mg, 0.44 mmol) were dissolved in toluene (8 mL) and 1-butanol (4 mL). Then the mixture was stirred for 10 h at 110 °C under an argon atmosphere. After reaction, the mixture was filtered under suction, washed with ethanol and then vacuum-dried to obtain the black product (65 mg): Yield 62%.^{1}H NMR (400 MHz, DMSO-d_6, ppm): δ 1.76-1.85 (m, 2H, -CH_2-), 2.20-2.27 (m ,2H, CH_2-), 2.55 (t, J = 6.9 Hz, 2H, -CH_2-), 2.60 (t, J = 5.5 Hz, 2H, -CH_2-), 2.71 (t, J = 5.2 Hz, 2H, -CH_2-), 5.00 (t, J = 7.3 Hz, 2H, -CH_2-), 6.62 (dd, J = 8.3 Hz, 2.3 Hz, 1H, Ph-H), 6.85 (d, J = 2.1 Hz, 1H), 6.90 (s, 1H, Ph-H), 7.18 (d, J = 8.4 Hz, 1H, Ph-H), 7.34 (d, J = 15.0 Hz, 1H, alkene-H), 7.88 (t, J = 7.8 Hz, 1H, Ph-H), 8.13 (t, J = 8.1 Hz, 1H, Ph-H), 8.34 (d, J = 6.8 Hz, 1H, Ph-H), 8.48 (d, J = 2.8 Hz, 1H, Ph-H), 8.51 (d, J = 15.3 Hz, 1H, alkene-H), 8.83 (d, J = 8.2 Hz, 1H, Ph-H), 9.00 (d, J = 6.8 Hz, 1H, Ph-H), 10.23 (s, 1H, -OH). HRMS (ESI-MS) m/z: calcd for $[C_{27}H_{25}NNaO_5]^+$: 498.1351, found: 498.1341.

Synthesis of QMC-OH-N

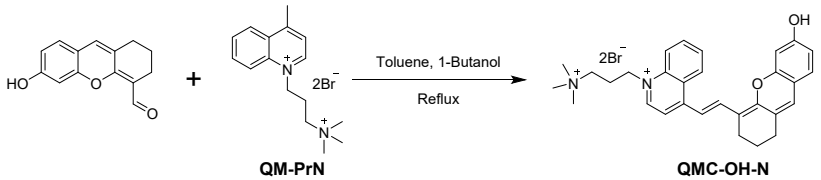

QM-PrN QMC-OH-N

Compound 3 (50 mg, 0.22 mmol) and QM-PrN (88 mg, 0.22 mmol) were dissolved in toluene (8 mL) and 1-butanol (4 mL). Then the mixture was stirred for 10 h at 110 °C under an argon atmosphere. After reaction, the mixture was filtered under suction, washed with ethanol and then vacuum-dried to obtain the black product (48 mg): Yield 64%.^{1}H NMR (400 MHz, DMSO-d_6, ppm): δ 1.78(t, J = 5.2 Hz, 2H, -CH_2-), 2.27-2.35 (m, 2H, -CH_2-), 2.35-2.42 (m, 2H, -CH_2-), 2.56 (t, J = 5.4 Hz, 2H, -CH_2-), 3.18 (s, 9H, -$C(CH_3)_3$), 3.47 3.54 (m, 2H, -CH_2-), 4.14 (t, J = 7.4 Hz, 2H, -CH_2-), 6.06 (d, J = 1.8 Hz, Ph-H), 6.42 (dd, J = 8.6 Hz, 2.0 Hz, 1H, Ph-H), 6.59 (s, 1H, Ph-H), 6.65 (d, J = 14.1 Hz, 1H, alkene-H), 6.79 (d, J = 8.6 Hz, 1H, Ph-H), 7.35 (d, J = 7.2 Hz, 1H, Ph-H), 7.47 (t, J = 7.6 Hz, 1H, Ph-H), 7.62 (d, J = 8.7 Hz, 1H, Ph-H), 7.71 (t, J = 7.8 Hz, 1H, Ph-H), 7.96 (d, J = 7.0 Hz, 1H, Ph-H), 8.10 (d, J = 14.0 Hz, 1H, alkene-H), 8.17 (d, J = 8.4 Hz, 1H, Ph-H). ^{13}C NMR (100 MHz, DMSO-d_6, ppm): δ 15.04, 20.35, 24.25, 28.74, 51.06, 102.18, 112.07, 112.11, 113.64, 114.13, 118.62, 125.86, 125.99, 126.30, 127.03, 127.84, 128.26, 134.46, 137.60, 137.66, 145.30, 152.38, 153.69, 154.44, 159.79. HRMS (ESI-MS) m/z: calcd for $[C_{30}H_{34}N_2O_2]^{2+}$: 227.1305, found: 227.1303.

Synthesis of PAB-Glu-Boc

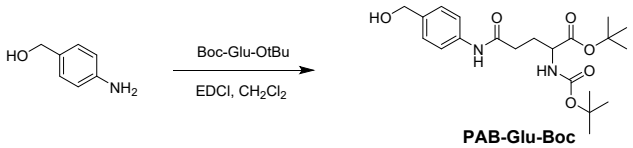

PAB-Glu-Boc

Boc-Glu-OtBu (1.21 g, 4.0 mmol) and EDCl (1.15 g, 6.0 mmol) were dissolved in dichloromethane (40 mL). 4-aminobenzyl alcohol (0.74 g, 6.0 mmol) was dissolved in 10 mL of dichloromethane and added to the reaction mixture at 0 °C. Then the mixture was stirred for 5 h at room temperature under an argon atmosphere, the solution color gradually changed from yellow to light red. After reaction, the mixture was washed with water and phase separation to collect the organic layer, the solvent was removed under reduced pressure. The crude product was purified by silica gel chromatography using ethyl acetate/methanol (v/v, 100:5) as the eluent to afford PAB-Glu-Boc

as a yellow solid (1.1 g): Yield 73 %. ^{1}H NMR (400 MHz, $CDCl_3$, ppm): δ 1.44 (s, 9H, -$C(CH_3)_3$), 1.45 (s, 9H, -$C(CH_3)_3$), 1.85 2.18 (m, 2H, -CH_2-), 2.40 (t, J = 6.6 Hz, 2H, -CH_2-), 2.89 (t, J, 1H, -OH), 4.17 (t, J = 6.4 Hz, 1H, -CONH-), 4.60 (s, 2H, -CH_2-), 5.46 (d, J = 8.0 Hz, 1H, -CONH-), 7.26 (d, J = 8.0 Hz, 2H, Ph-H), 7.52 (d, J = 7.8 Hz, 2H, Ph-H), 8.92 (s, 1H, -CONH-). ^{13}C NMR (100 MHz, $CDCl_3$, ppm): δ 28.00, 28.36, 29.98, 33.41, 53.74, 64.66, 80.34, 82.58, 120.23, 127.68, 136.75, 137.60, 156.40, 170.95, 171.41. HRMS (ESI-MS) m/z: calcd for $[C_{21}H_{32}N_2NaO_6]^+$: 431.2158, found: 431.2146.

Synthesis of Br-Glu-Boc

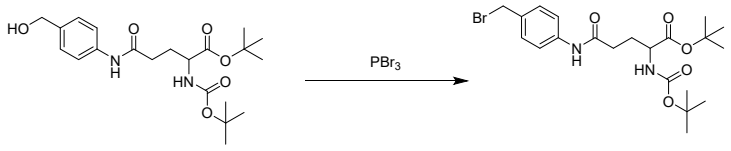

PAB-Glu-Boc (400 mg, 0.98 mmol) was dissolved in tetrahydrofuran (8 mL). PBr_3 (406 mg, 1.5 mmol) was dissolved in 2 mL of tetrahydrofuranand added to the reaction mixture at 0 °C. Then the mixture was stirred for 2 h under an argon atmosphere. After reaction, a saturated sodium bicarbonate solution was added to adjust the pH to approximately 7. The mixture was extracted with ethyl acetate. The combined ethyl acetate extracts were washed with water and dried (Na_2SO_4). The solvent was removed under reduced pressure, and then the crude product was purified by silica gel chromatography using petroleum ether/ethyl acetate (v/v, 2:1) as the eluent to afford Br-Glu-Boc as a white solid (150 mg): Yield 37%. ^{1}H NMR (400 MHz, $CDCl_3$, ppm): δ 1.46 (d, J = 4.8 Hz, 18H, -C(CH_3)$_3$), 1.89-2.29 (m, 2H, -CH_2-), 2.43-2.47 (m, 2H, -CH_2-), 4.22 (t, J = 7.2 Hz, 1H, -CH-), 4.49 (s, 2H, -CH_2-), 5.45 (d, J = 8.0 Hz, 1H, -CONH-), 7.34 (d, J = 8.4 Hz, 2H, Ph-H), 7.61 (d, J = 8.4 Hz, 2H, Ph-H), 9.14 (s, 1H, -CONH-).

Synthesis of Glu-Boc-DDAO

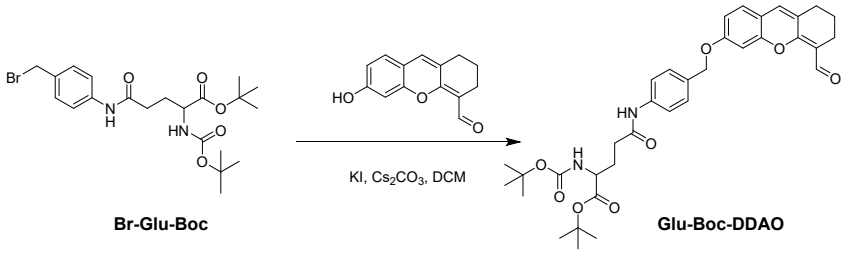

Br-Glu-Boc (200 mg, 0.35 mmol), Cs_2CO_3 (1.1 g, 3.45 mmol) and KI (120 mg, 0.69 mmol) were dissolved in dichloromethane (10 mL). Compound 3 (60 mg, 0.23 mmol) was dissolved in 5 mL of dichloromethane added to the reaction mixture. Then the mixture was stirred for 16 h under at room temperature an argon atmosphere. After reaction, the mixture was filtered through celite to remove insoluble materials. The crude product was purified by silica gel chromatography using petroleum ether/ethyl acetate (v/v, 4:1) as the eluent to afford Glu-Boc-DDAO as a yellow solid (40 mg): Yield 18 %. ^{1}H NMR (400 MHz, $CDCl_3$, ppm): δ 1.39 (d, J = 6.8 Hz, 18H, -C(CH_3)$_3$), 1.64-1.60 (m, 2H, -CH_2-), 1.84-2.03 (m, 2H, -CH_2-), 2.29 (t, J = 6.0 Hz, 2H, -CH_2-), 2.20 (t, J = 7.6 Hz, 4H), 4.13-4.17 (m, 1H, -CH-), 4.97 (s, 2H, -CH_2-), 5.34 (d, J = 8.0 Hz, 1H, -CH_2-), 6.57 (s, 1H, CONH-), 6.64 (d, J = 8.0 Hz, 2H, Ph-H), 7.00 (d, J = 8.4 Hz, 1H, Ph-H), 7.30 (d, J = 8.0 Hz, 2H, Ph-H), 7.59 (d, J = 8.4 Hz, 2H, Ph-H), 9.02 (s, 1H, -CONH-), 10.22(s, 1H, -CHO). ^{13}C NMR (100 MHz, $CDCl_3$, ppm): δ 9.58, 10.39, 24.98, 118.09, 122.27, 124.37, 126.16, 128.11, 131.22, 132.67, 135.04, 146.31, 148.05. HRMS (ESI-MS) m/z: calcd for $[C_{35}H_{43}N_2O_8]^+$: 619.3019, found: 619.3004.

Synthesis of QM-C-GGT-Boc

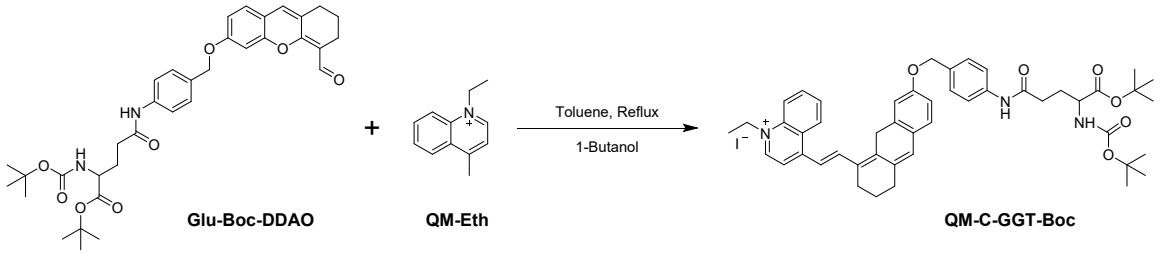

Glu-Boc-DDAO (46 mg, 0.08 mmol) and QM-Eth (196 mg, 0.74 mmol) were dissolved in toluene (4 mL) and 1-butanol (2 mL). Then the mixture was stirred for 12 h under at 110 °C an argon atmosphere. After reaction, the solvent was removed under reduced pressure. The crude product was purified by silica gel chromatography using dichloromethane/methanol (v/v, 100:3) as the eluent to afford QM-C-GGT-Boc as a deep blue solid (47 mg): Yield 65 %. ^{1}H-NMR (400 MHz, CD_3OD, ppm): δ 1.44 (s, 9H), 1.48 (s, 9H), 1.56 (t, J = 7.0 Hz, 3H, CH_3), 1.75-1.83 (m, 2H, -CH_2-), 1.91-1.23 (m, 2H, -CH_2-), 2.42-2.51 (m, 4H, -CH_2-), 2.52-2.59 (m, 2H, -CH_2-), 4.05-4.10 (m, 1H, -CH-), 4.56-4.67 (m, 2H, -CH_2-), 5.03 (s, 2H, -CH_2-), 6.51 (s, 1H, alkene-H), 6.64 (d, J = 8. Hz, 1H, Ph-H), 6.97 (d, J = 8.5 Hz, 1H, Ph-H), 7.01 (d, J = 15.3 Hz, 1H, alkene-H), 7.06 (s, 1H, -CONH-), 7.25 (d, J = 7.7 Hz, 2H, Ph-H), 7.35 (d, J = 8.0 Hz, 1H, Ph-H), 7.42 (d, J = 7.9 Hz, 2H, Ph-H), 7.48 (d, J = 8.0 Hz, 1H, Ph-H), 7.77 (t, J = 7.8 Hz, 1H, Ph-H), 8.01 (t, J = 7.2 Hz, 1H, Ph-H), 8.09 (d, J = 8.7 Hz, 1H, Ph-H), 8.26 (d, J = 6.8 Hz, 1H, Ph-H), 8.38 (d, J = 14.8 Hz, 1H, alkene-H), 8.47 (d, J = 8.4 Hz, 1H, Ph-H), 8.66 (d, J = 6.6 Hz, 1H, -CONH-). ^{13}C-NMR (100 MHz, CD_3OD, ppm): δ 14.29, 20.05, 24.71, 28.46,33.88, 35.83, 53.14, 55.78, 62.69, 64.12, 68.13, 80.58, 82.81, 102.02, 113.77, 116.73, 120.09, 126.95, 128.02, 132.79, 135.53, 138.78, 145.10, 153.86, 155.07, 156.76, 158.25, 161.71, 172.62, 173.53. HRMS (ESI-MS) m/z: calcd for $[C_{47}H_{54}N_3O_7]^+$: 772.3957, found: 772.3947.

Synthesis of QM-SO_3-GGT-Boc

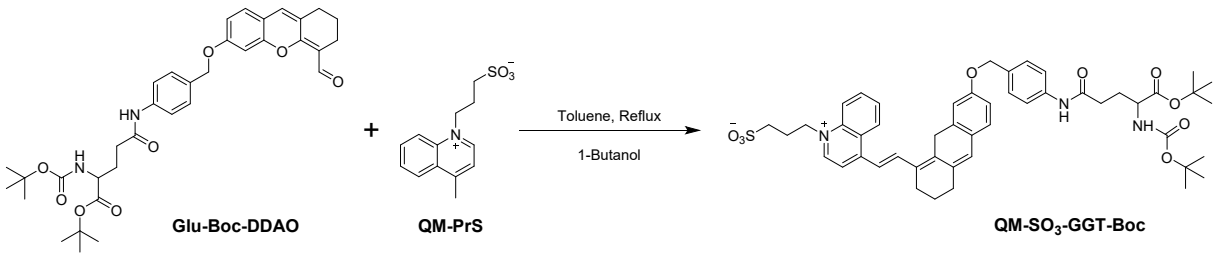

Glu-Boc-DDAO (46 mg, 0.08 mmol) and QM-PrS (212mg, 0.8 mmol) were dissolved in toluene (4 mL) and 1-butanol (2 mL). Then the mixture was stirred for 12 h under at 110 °C an argon atmosphere. After reaction, the solvent was removed under reduced pressure. The crude product was purified by silica gel chromatography using dichloromethane/methanol (v/v, 100:3) as the eluent to afford QM-SO_3-GGT-Boc as a deep blue solid (60 mg): Yield 71 %. ^{1}H-NMR (400 MHz, DMSO-d_6, ppm): δ 1.38 (s, 9H, -C(CH_3)$_3$), 1.40 (s, 9H, -C(CH_3)$_3$), 1.79-1.81 (m, 2H, -CH_2-), 1.98-2.04 (m, 2H, -CH_2-), 2.24 (t, J = 7.2 Hz, 2H, -CH_2-), 2.41 (t, J = 8.8 Hz, 2H, -CH_2-), 2.54 (s, 2H, -CH_2-), 2.63 (d, J = 6.8 Hz, 2H, -CH_2-), 2.69 (s, 2H, -CH_2-), 3.34-3.87 (m, 1H, -CH-), 4.99 (d, J = 7.2 Hz, 2H, -CH_2-), 5.01 (s, 2H, -CH_2-), 6.80 (d, J = 14.4 Hz, 1H, alkene-H), 6.84 (s, 1H, alkene-H), 7.16 (s, 2H, Ph-H), 7.23 (d, J = 8.4 Hz, 1H, Ph-H), 7.40 (s, 1H, Ph-H), 7.42 (s, 2H, Ph-H), 7.62 (d, J = 8.8 Hz, 2H, Ph-H), 7.87 (t, J = 7.2 Hz, 1H, Ph-H), 8.11 (t, J = 8.0 Hz, 1H, Ph-H), 8.30 (d, J = 6.8 Hz, 1H, -CONH-), 8.45 (s, 1H, Ph-H), 8.48 (d, J = 14.3 Hz, 1H,

alkene-H), 8.79 (d, J = 8.8 Hz, 1H, Ph-H), 9.02 (d, J = 6.8 Hz, 1H, Ph-H), 10.02 (s, 1H, -CONH-). HRMS (ESI-MS) m/z: calcd for $[C_{48}H_{56}N_3O_{10}S]^+$: 866.3686, found: 866.3696.

Synthesis of QM-N-GGT-Boc

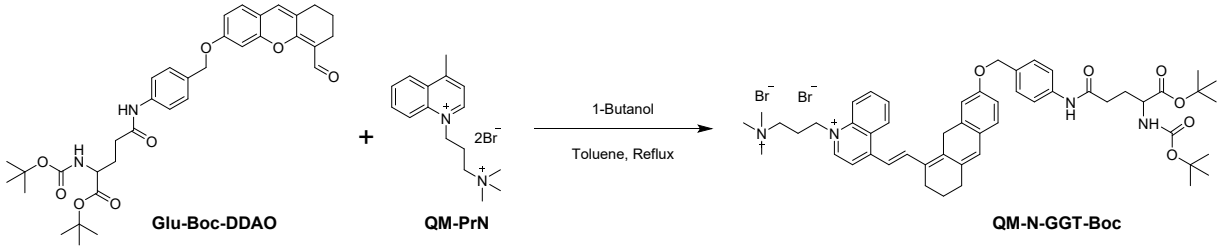

Glu-Boc-DDAO QM-PrN QM-N-GGT-Boc

Glu-Boc-DDAO (46 mg, 0.08 mmol) and QM-PrN (196 mg, 0.74 mmol) were dissolved in toluene (4 mL) and 1-butanol (2 mL). Then the mixture was stirred for 12 h under at 110 °C an argon atmosphere. After reaction, the solvent was removed under reduced pressure. The crude product was purified by silica gel chromatography using dichloromethane/methanol (v/v, 100:3) as the eluent to afford QM-N-GGT-Boc as a deep blue solid (60 mg): Yield 75 %. ^{1}H-NMR (400 MHz, CD_3OD, ppm): δ 1.48 (s, 9H, -C(CH_3)$_3$), 1.52 (s, 9H, -C(CH_3)$_3$), 1.68-1.74 (m, 2H, -CH_2-), 1.91-2.22 (m, 2H, -CH_2-), 2.33 (m, 4H, -CH_2-), 2.49 (t, J = 8.8 Hz, 4H, -CH_2-), 3.27 (s, 9H, -N(CH_3)$_3$), 3.73 (t, J = 8.0 Hz, 2H, -CH_2-), 4.06-4.10 (m, 1H, -CH-), 4.54 (s, 2H, -CH_2-), 4.73 (s, 2H, -CH_2-), 6.35 (s, 1H, alkene-H), 6.48 (d, J = 8.4 Hz, 1H, Ph-H), 6.68 (d, J = 15.0 Hz, 1H, alkene-H), 6.83 (d, J = 8.4 Hz, 2H, Ph-H), 6.90 (d, J = 8.4 Hz, 2H, Ph-H), 7.13 (d, J = 8.4 Hz, 2H, Ph-H), 7.66 (t, J = 8.6 Hz, 1H, Ph-H), 7.93 (d, J = 8.2 Hz, 1H , Ph-H), 7.97 (d, J = 7.3 Hz, 1H, Ph-H), 8.06 (d, J = 8.4 Hz, 1H, Ph-H), 8.09 (d, J = 14.2 Hz. 1H, alkene-H), 8.23 (d, J = 8.7 Hz, 1H, Ph-H), 8.69 (d, J = 8.4 Hz, 1H, Ph-H). ^{13}C-NMR (100 MHz, CD_3OD, ppm): δ 14.29, 20.05, 24.71, 28.46, 32.88, 35.83, 53.14, 55.78, 62.69, 64.12, 68.13, 80.58, 82.81, 102.02, 113.77, 116.73, 120.09, 126.95, 127.26, 128.02, 129.07, 132.79, 135.53, 138.78, 139.12, 145.10, 153.86, 155.07, 158.25, 161.71, 172.62, 173.53. HRMS (ESI-MS) m/z: calcd for $[C_{51}H_{64}N_4O_7]^{2+}$: 422.2382, found: 422.2364.

Synthesis of QMC-C-GGT

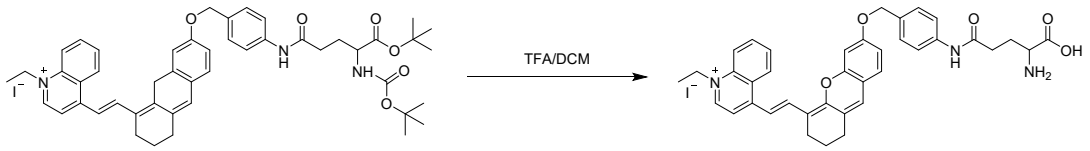

QM-C-GGT-Boc QMC-C-GGT

QM-C-GGT-Boc (50 mg, 0.06 mmol) was dissolved in dichloromethane, then added trifluoroacetic acid (5 mL). Then the mixture was stirred for 12 h under at room temperature under an argon atmosphere. After reaction, the mixture was washed with dichloromethane three times. The solvent was removed under reduced pressure to afford the product as a black solid (18 mg): Yield 43%. ^{1}H-NMR (400 MHz, DMSO-d_6, ppm): δ 1.54 (s, 3H, -CH_3), 1.79 (s, 2H, -CH_2-), 2.11 (s, 3H, -CH_2-, -CH-), 2.56 (s, 4H, -CH_2-), 2.70 (s, 2H, -CH_2), 3.86 (s, 2H, -NH_2), 4.88 (s, 2H, CH_2-), 5.12 (s, 2H, -CH_2-), 6.81 (d, J = 8.0 Hz, 1H, Ph-H), 6.85 (s, 1H, Ph-H), 7.15 (s, 1H, alkene-H), 7.23 (d, J = 8.4 Hz, 1H, Ph-H), 7.32 (d, J = 14.8 Hz, 1H, alkene-H), 7.41 (d, J = 8.0 Hz, 2H, Ph-H), 7.65 (d, J = 7.6 Hz, 2H, Ph-H), 7.88 (s, 1H, Ph-H), 8.14 (s, 2H, Ph-H), 8.35 (m, 1H, alkene-H), 8.37 (s, 1H, -CONH-), 8.48 (d, J = 8.2 Hz, 1H, Ph-H), 8.81 (d, J = 8.0 Hz, 1H, Ph-H), 9.05 (d, J = 4.8 Hz, 1H, Ph-H), 10.24 (s, 1H, -COOH). ^{13}C-NMR (100 MHz,

DMSO-d_6, ppm): δ 15.18, 19.60, 52.47, 119.19, 122.80, 127.17, 129.90, 135.07, 158.38. HRMS (ESI-MS) m/z: calcd for $[C_{38}H_{38}N_3O_5]^+$: 616.2806, found: 616.2811.

Synthesis of QMC-SO_3-GGT

QM-SO_3-GGT-Boc **QMC-SO_3-GGT**

QM-SO_3-GGT-Boc (50 mg, 0.06 mmol) was dissolved in dichloromethane (5 mL), then added trifluoroacetic acid (5 mL). Then the mixture was stirred for 12 h under at room temperature under an argon atmosphere. After reaction, the mixture was added dichloromethane, then solvent was removed under reduced pressure. The product was purified by thermal recrystallization dichloromethane/methanol (v/v, 5:1) to afford compound QMC-SO_3-GGT as a black solid (16 mg): Yield 43 %. ^{1}H-NMR (400 MHz, DMSO-d_6, ppm): δ 1.77-1.85 (m, 2H, -CH_2-), 1,93-2.15 (m, 2H, CH_2-), 2.24 (t, J = 7.2 Hz, 2H, -CH_2-), 2.55-2.60 (m, 4H, -CH_2-), 2.71 (t, J = 6.4 Hz, 2H, -CH_2-), 3.45-3.51 (m, 2H, -CH_2-), 3.59 (t, J = 6.6 Hz, 1H, -CH-), 5.01 (t, J = 6.4 Hz, 2H, -CH_2-), 5.11 (s, 2H, -CH_2-), 6.81 (dd, J = 2.0 Hz, 8.4 Hz, alkene-H), 6.91 (s, 1H, alkene-H), 7.16 (s, 1H, Ph-H), 7.27 (d, J = 8.5 Hz, 1H, Ph-H), 7.36 (d, J = 8.0 Hz, 2H, Ph-H), 7.40 (d, J = 14.4 Hz, 1H, alkene-H), 7.64 (d, J = 8.5 Hz, 2H, Ph-H), 7.89 (t, J = 7.6 Hz, 1H, Ph-H), 8.13 (t, J = 8.0 Hz, 1H, Ph-H), 8.32 (d, J = 6.4 Hz, 1H, Ph-H), 8.48 (s, 1H, -CONH-), 8.51 (d, J = 8.8 Hz, 1H, Ph H), 8.85 (d, J = 8.4 Hz, 1H, Ph-H), 9.03 (d, J = 6.4 Hz, 1H, Ph-H), 10.22 (s, 1H, -COOH). HRMS (ESI-MS) m/z: calcd for [C39H40N3SO8]+: 710.2536, found: 710.2534.

Synthesis of QMC-N-GGT

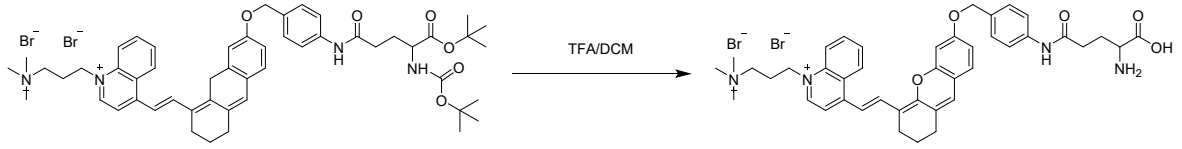

QM-N-GGT-Boc **QMC-N-GGT**

QM-N-GGT-Boc (50 mg, 0.05 mmol) was dissolved in dichloromethane (5 mL), then added trifluoroacetic acid (5 mL). Then the mixture was stirred for 12 h under at room temperature under an argon atmosphere. After reaction, the mixture was added dichloromethane, then solvent was removed under reduced pressure. The crude product was purified by C18 reverse-phase silica column using water/methanol/water(v/v, 4:1) as the eluent to afford QMC-N-GGT as a deep blue solid (15 mg): Yield 35 %. ^{1}H-NMR (400 MHz, CD_3OD, ppm): δ 1.83 (s, 2H, -CH2-), 2.16 (d, J = 7.2 Hz, 2H, -CH_2-), 2.51 (s, 4H, -CH_2-), 2.59 (s, 4H, -CH_2-), 3.20 (s, 9H, -$N(CH_3)_3$), 3.63 (s, 3H, -CH_2-, -CH-), 4.70 (s, 2H, -CH_2-), 4.86 (s, 2H, -CH_2-), 6.63 (s, 1H, alkene-H), 6.68 (d, J = 14.0 Hz, 1H, alkene-H), 6.88 (s, 1H, Ph-H), 7.05 (d, J = 8.4 Hz, 2H, Ph-H), 7.09 (d, J = 8.0 Hz, 2H, Ph-H), 7.22 (d, J = 7.6 Hz, 2H, Ph-H), 7.81 (t, J = 7.6 Hz, 1H, Ph-H), 7.98 (d, J = 6.4 Hz, 1H, Ph-H), 8.07 (t, J = 8.0 Hz, 1H, Ph-H), 8.17 (d, J = 8.4 Hz, 1H, Ph-H), 8.36 (d, J = 14.6 Hz, 1H, alkene-H), 8.51 (d, J = 8.2 Hz, 1H, Ph-H), 8.72 (d, J = 8.6 Hz, 1H, Ph-H). ^{13}C-NMR (100 MHz, CD_3OD, ppm): δ 21.40, 24.33, 25.18, 27.65, 30.08, 33.63, 53.15, 63.94, 69.99, 101.76, 102.92, 112.90, 113.39, 116.66, 118.77, 119.66, 120.08, 126.73, 127.31, 128.12, 129.13, 132.72, 135.74, 138.71, 139.13, 145.15, 154.15,

156.73, 161.68, 162.88, 163.18, 172.72. HRMS (ESI-MS) m/z: calcd for $[C_{42}H_{48}N_4O_5]^{2+}$: 344.1807, found: 344.1803.

Cell experiment

Cell lines

The human hepatocellular carcinoma cell line HepG2 and 293T cell were purchased from the Institute of Cell Biology (Shanghai, China). Cells were all propagated in T-25 flasks cultured at 37 °C under a humidified 5 % CO_2 atmosphere in DMEM medium (GIBCO/Invitrogen, Camarillo, CA, USA), which were supplemented with 10 % fetal bovine serum (FBS, Biological Industry, Kibbutz Beit Haemek, Israel) and 1 % penicillin-streptomycin (Solarbio life science, Beijing, China).

***In vitro* cytotoxicity assay**

The cytotoxicity of the probe QMC-N-GGT to HepG 2 and 293 T cells were studied by standard MTT assays. 2 × 10^4 cells/mL cells were seeded in 96-well plates and then incubated with various concentrations of QMC-N-GGT for 24 h. After that, 10 μL of MTT (5 mg/mL) was added to each well and incubated for another 4 h. Finally, the media was discharged, and 100 μL of DMSO was added to dissolve the formazan crystals. The plate was shaken for about 10 min, and each well was analyzed by the microplate reader and detected at the absorbance of 490 nm. The cell viability (%) = (OD_{sample}-OD_{blank}) / ($OD_{control}$- OD_{blank}k) × 100%. OD_{sample}, $OD_{control}$, and OD_{blank} denote the cells incubated with various of concentrations of the probe, the cells without the probe, and the wells containing only the culture media, respectively.

***In vitro* cellular imaging**

The HepG 2 cells at 1×10^5 cells well were seeded onto glass-bottom petri dishes with complete medium (1.5 mL) for 12 h. Then the cells pre-incubated with and without GGstop (GGT inhibitor) were respectively exposed to QMC-N-GGT for different time. PBS was used to wash cells for three times to clean the background. 4 % paraformaldehyde was added at 37 °C for 20 min. The fixed cells were rinsed with PBS twice. The images were then photographed by using a Leica TCS SP8 (63 × oil lens) with 770 nm as the excitation wavelength and 800-850 as the emission wavelength.

Animals

All schistosome-infected mouse models required for the experiments were standardized and provided by the National Institute of Parasitic Diseases, Chinese Center for Disease Control and Prevention. All experiments involving critical host snails (Oncomelania hupensis) were conducted in biosafety level 2 laboratory environments by professionally trained technicians following standardized operating procedures.

The experimental mice were Balb/C mouse, (12–15 g, female and 20–30 g, male) were provided by the Laboratory Animal Research Center of the National Institute of Parasitic Diseases at Chinese Center for Disease Control and Prevention, Chinese Center for Tropical Diseases Research, National Research Center for Tropical Diseases (Shanghai, China). Male mice were infected with Schistosomiasis mansoni cercaria and kept for 50 days. Female mice served as controls and were not infected.

Mouse model of *Schistosoma mansoni* infection

The schistosomiasis mouse model was established according to the following procedure:

1. Parasite preparation: cercariae were shed from infected intermediate snail hosts by exposure to artificial light (26-28 °C) for 1-2 h. The concentration was determined by averaging counts from three 10-μL aliquots under a light microscope to ensure an accurate infection dose.

2. Animal infection: healthy mice were used as definitive hosts. One day post-depilation, anesthetized mice were infected percutaneously by exposing the abdominal skin to a cercarial suspension for 20-30 min to allow active larval penetration.

3. Model validation: following skin penetration, larvae migrate to the hepatic portal system, where mature worms pair and produce eggs by 4-5 weeks post-infection. Successful infection was confirmed via fecal egg counts or serum antigen detection. Probing experiments were conducted at 7-8 weeks post-infection to target the peak of egg-induced granuloma formation.

Real-time *in vivo* fluorescence imaging in tumor-bearing mice

QMC-N-GGT (administered at a QMC-N-GGT dose of 3 μmol kg-1) in PBS were intravenously injected via tail vein into theschistosome-infected mice. The real-time in vivo imaging was photographed at the different time by using a PerkinElmer IVIS Lumina Kinetic Series III imaging system with 620 nm and 770 nm separately as the dual-channel excitation wavelength and 700-760 nm and 800-850 as the dual-channel emission wavelength. After injection, the mice were sacrificed at 24 h. The major organs, including kidney, lung, spleen, liver, and heart were excised and washed with 0.9% saline. The optical images of the organs and tissues were taken using a PE in vivo Professional Imaging System as described above.

2. Solvatochromism and environmental sensitivity of QMC series

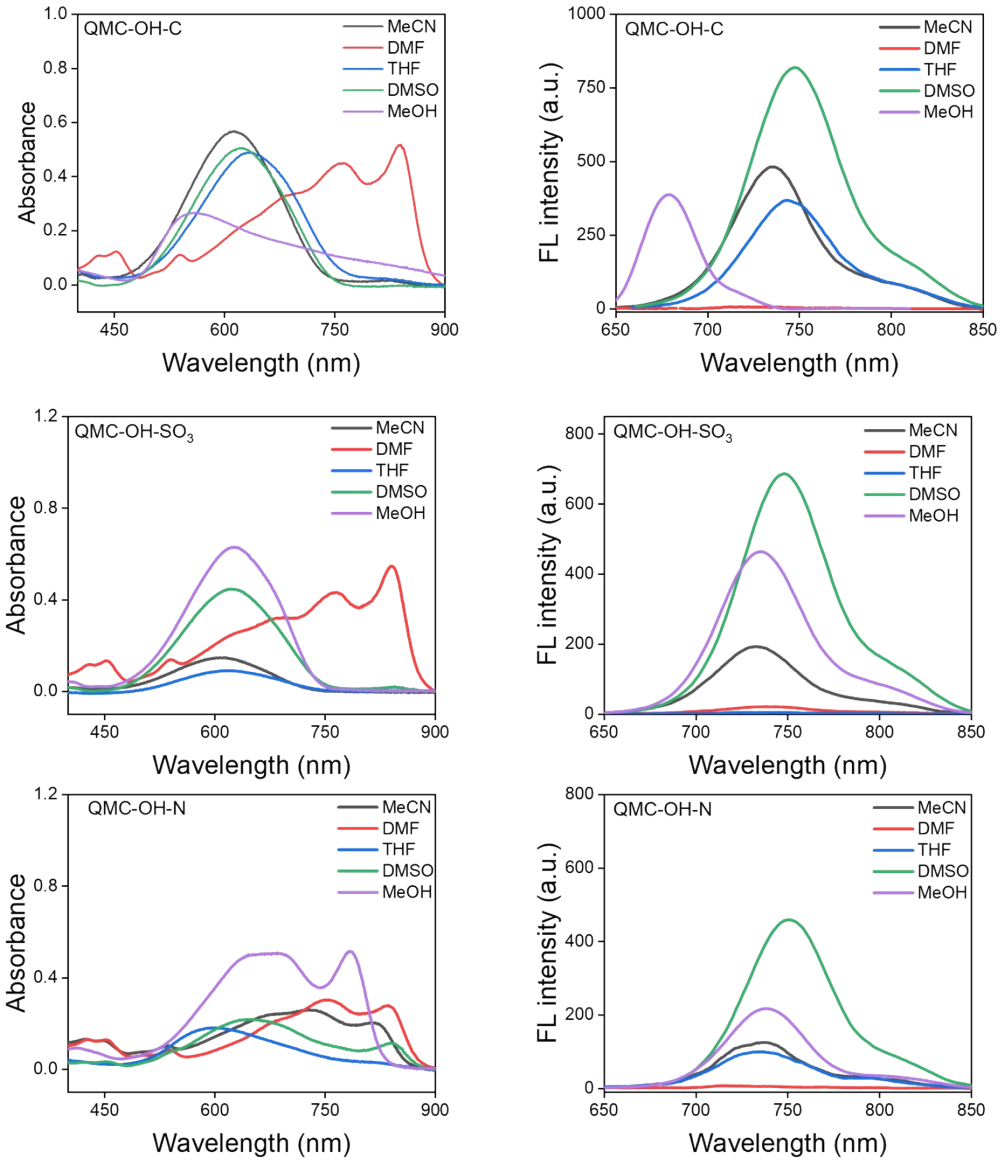

Fig. S1 Absorption (left) and fluorescence (right) spectra of QMC-OH-C, QMC-OH-SO_3, and QMC-OH-N (10 μM, λ_{ex} = 620 nm) recorded in various organic solvents of varying polarities and protic/aprotic natures. The QMC series exhibits characteristic solvatofluorochromic shifts, reflecting the sensitivity of the internal charge transfer (ICT) process to the localized dielectric environment. Notably, the cationic probe QMC-OH-N demonstrates enhanced spectral stability and a reduced tendency for non-specific fluorescence enhancement in protic environments compared to its anionic and zwitterionic counterparts.

3. Absorption spectral response of QMC-OH-N toward pH variations

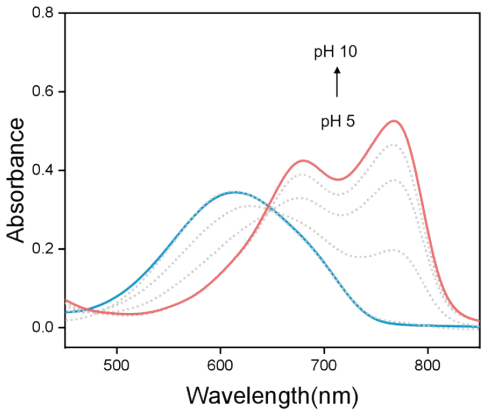

Fig. S2 UV-vis absorption spectra of QMC-OH-N (10 μM) in PBS with pH values ranging from 5.0 to 10.0

4. Solvatochromism and aqueous dispersibility of QMC-OH-N

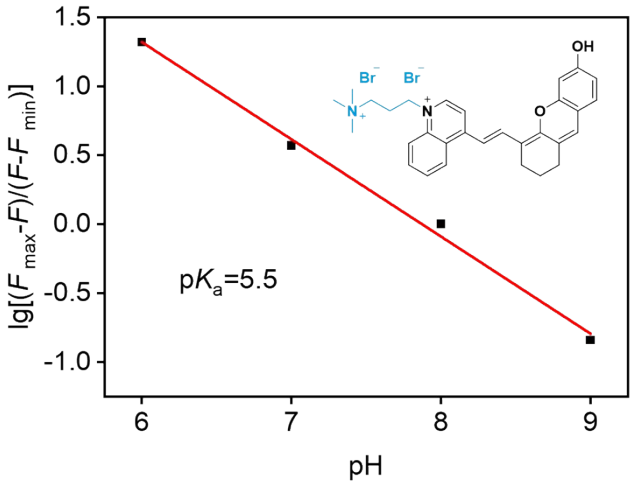

Fig. S3 Determination of the pK_a value for the enzymatic product QMC-OH-N. The pK_a of the released fluorophore QMC-OH-N was calculated to be 5.5 based on the linear regression of lg [(F_{max}- F)/ (F- F_{min})] versus pH values. This relatively low pK_a value confirms that the fluorophore predominantly exists in its deprotonated state at physiological pH (7.4), providing a robust fluorescence signal independent of subtle environmental pH fluctuations during *in vivo* imaging.

5. Solvatochromism and aqueous dispersibility of QMC-GGT probes

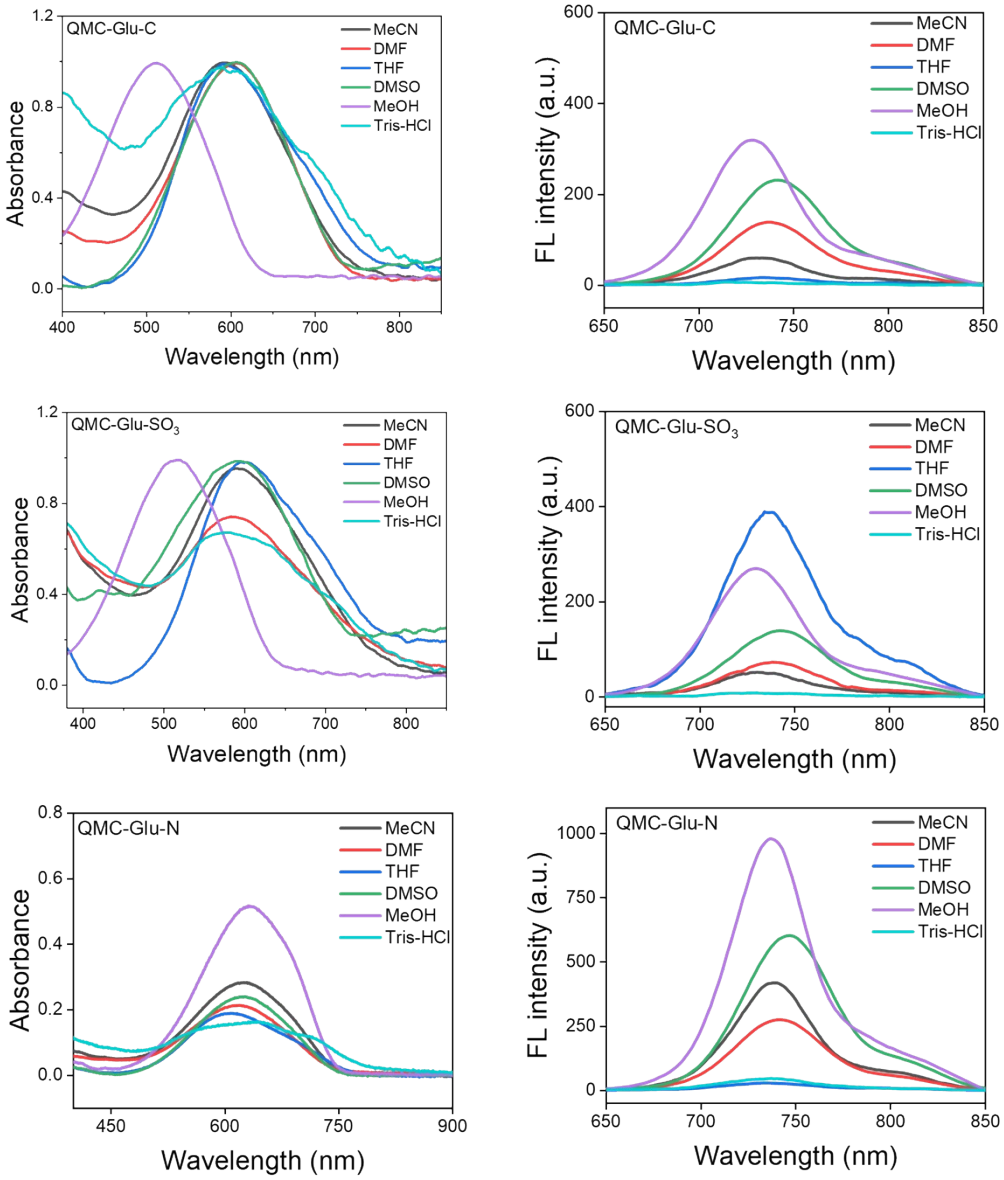

Fig. S4 Absorption (left) and fluorescence (right) spectra of QMC-C-GGT, QMC-SO_3-GGT, and QMC-N-GGT (10 μM ,λ_{ex} = 620 nm) recorded in various organic solvents with different polarities and aqueous buffer. The QMC-Glu series exhibits characteristic solvatofluorochromic shifts, confirming the sensitivity of the internal charge transfer (ICT) process to the localized dielectric environment. Notably, in the aqueous Tris-HCl environment, the cationic probe QMC-N-GGT displays significantly higher fluorescence intensity and superior spectral stability compared to the anionic (QMC-C-GGT) and zwitterionic (QMC-SO_3-GGT) derivatives.

6. Photostability evaluation of QMC-N-GGT

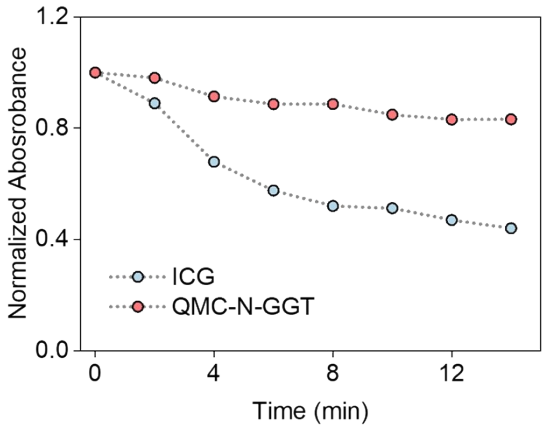

Fig. S5 Photostability evaluation of QMC-N-GGT. The photostability of QMC-N-GGT was assessed by monitoring the changes in normalized absorbance under continuous irradiation for 14 min, with the clinically used fluorophore ICG serving as a control. Upon sustained exposure, QMC-N-GGT maintained over 80% of its initial absorbance, whereas the signal of ICG rapidly decayed to approximately 40%. These results demonstrate the superior optical robustness of QMC-N-GGT against photobleaching, ensuring its reliability for persistent and high-fidelity biological imaging.

7. Biocompatibility and pharmacological safety evaluation of QMC-N-GGT

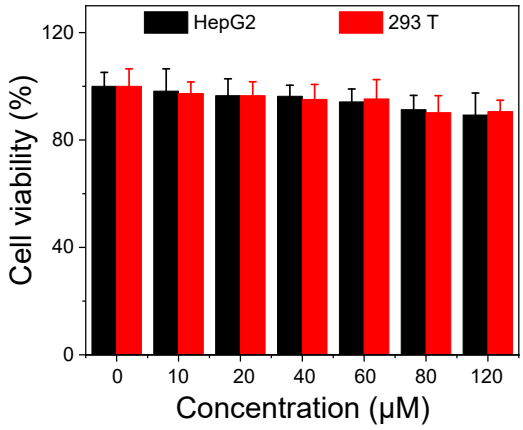

Fig. S6 Cell viability of HepG2 and 293T cells after incubation with various concentrations of QMC-N-GGT (0, 10, 20, 40, 60, 80, and 120 μM) for 24 h, as determined by the standard MTT assay. The results demonstrate that cell viability remains above 90% across the entire concentration range tested, even at the highest dosage of 120 μM. Data are expressed as mean ± s.d. (n = 6).

8. Evaluation of cell retention capability for probes with different charge regulation

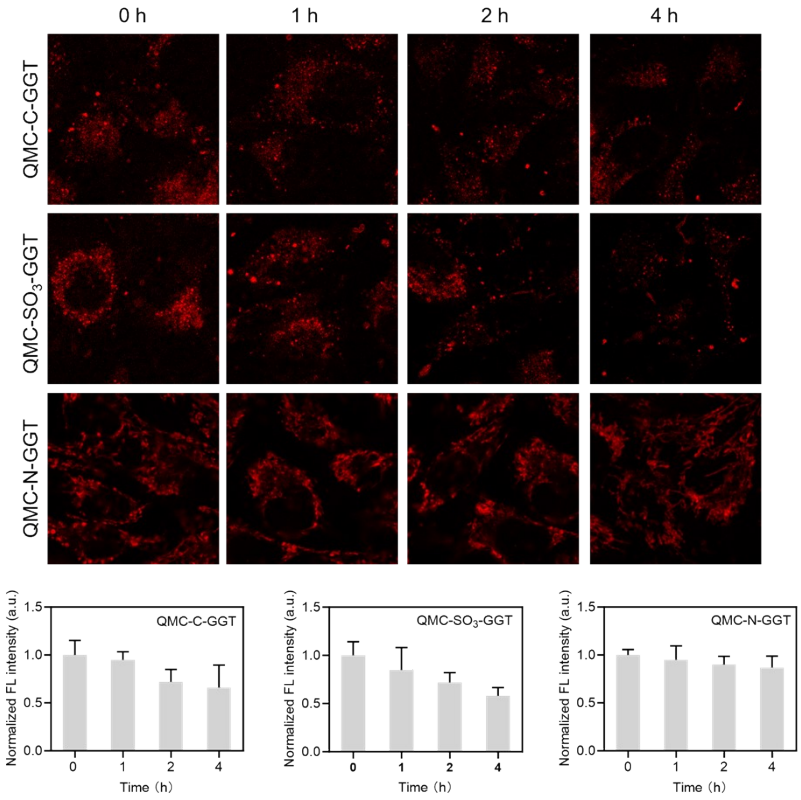

Fig. S7 Evaluation of cell retention capability for probes with different charge regulations. Intracellular fluorescence stability of QMC-C-GGT, QMC-SO_3-GGT, and QMC-N-GGT was quantitatively analyzed in HepG2 cells using confocal laser scanning microscopy (CLSM). After incubation with the respective probes, the cells were washed and maintained in fresh medium, followed by imaging at 0, 1, 2, and 4 h. The dicationic probe QMC-N-GGT exhibited superior signal retention (> 85% of initial intensity) over 4 h, whereas the QMC-C-GGT and QMC-SO_3-GGT showed significant signal decay.

9. Subcellular localization of QMC-N-GGT

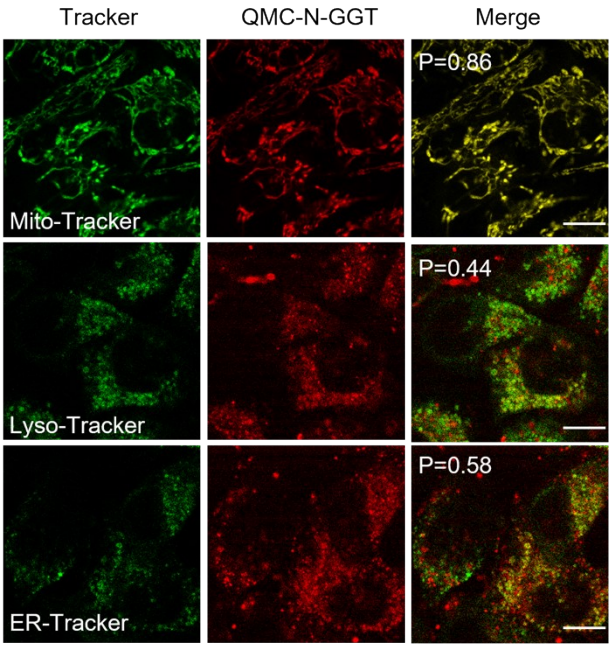

Fig. S8 Subcellular localization of QMC-N-GGT in HepG2 cells. Confocal fluorescence images of HepG2 cells co-stained with QMC-N-GGT (red channel) and various organelle trackers (green channel). The merged images and Pearson's correlation coefficients (P) demonstrate that QMC-N-GGT primarily localizes in the mitochondria (P = 0.86), while showing significantly lower overlap with lysosomes (P = 0.44) and the endoplasmic reticulum (P = 0.58). This mitochondrial targeting is attributed to the high mitochondrial membrane potential and the dicationic nature of the probe. Scale bars: 20 μm.

10. pH stability of QMC-N-GGT in reference channel

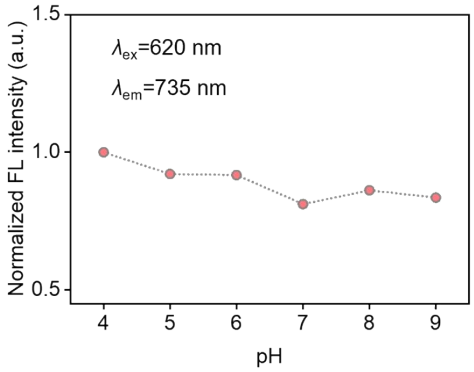

Fig. S9 pH stability of the reference signal (Channel 1). The stability of the fluorescence intensity of QMC-N-GGT (reference signal, λ_{ex} = 620 nm, λ_{em} = 735 nm) was evaluated across a wide physiological pH range (4.0–9.0). The normalized fluorescence intensity remained highly consistent, showing negligible fluctuations even under acidic or basic conditions.

11. Zeta potential and protein corona evaluation

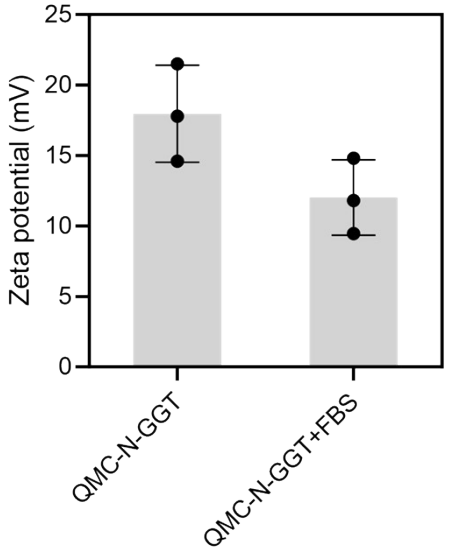

Fig. S10 Zeta potential and protein corona evaluation. Zeta potential measurements of QMC-N-GGT before and after incubation with 50% fetal bovine serum (FBS). The probe initially exhibited a high positive charge. Upon exposure to 50% FBS, the zeta potential decreased due to the formation of a protein corona. Notably, the probe maintained a significantly positive surface charge despite protein adsorption, suggesting that the dicationic scaffold remains effective in driving electrostatic-mediated cellular uptake and tissue accumulation in vivo. Data are presented as mean ± SD (n = 3).

12. Systemic pathological evaluation and pharmacological safety of QMC-N-GGT.

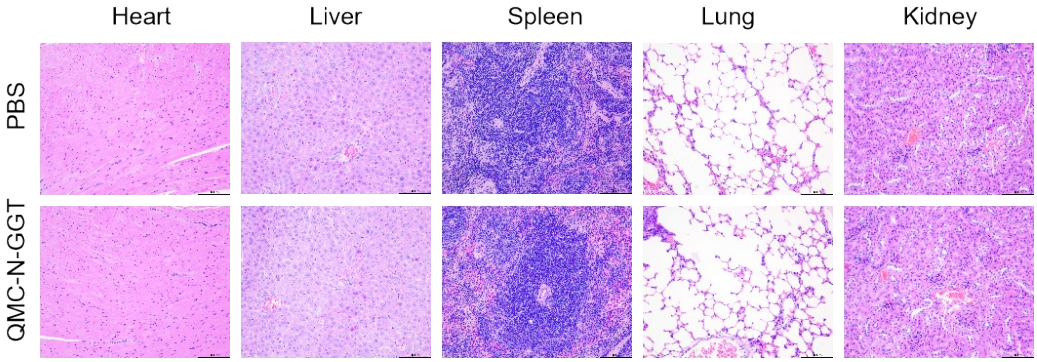

Fig. S11 Representative hematoxylin and eosin (H&E) stained images of major organs, including the heart, liver, spleen, lung, and kidney, harvested from mice at 24 h post-intravenous administration of PBS (control) or QMC-N-GGT. No discernible tissue damage, inflammatory infiltration, or morphological abnormalities were observed in the QMC-N-GGT treated group compared to the PBS control.

13. Characterization of intermediate compounds and QMC-N-GGT

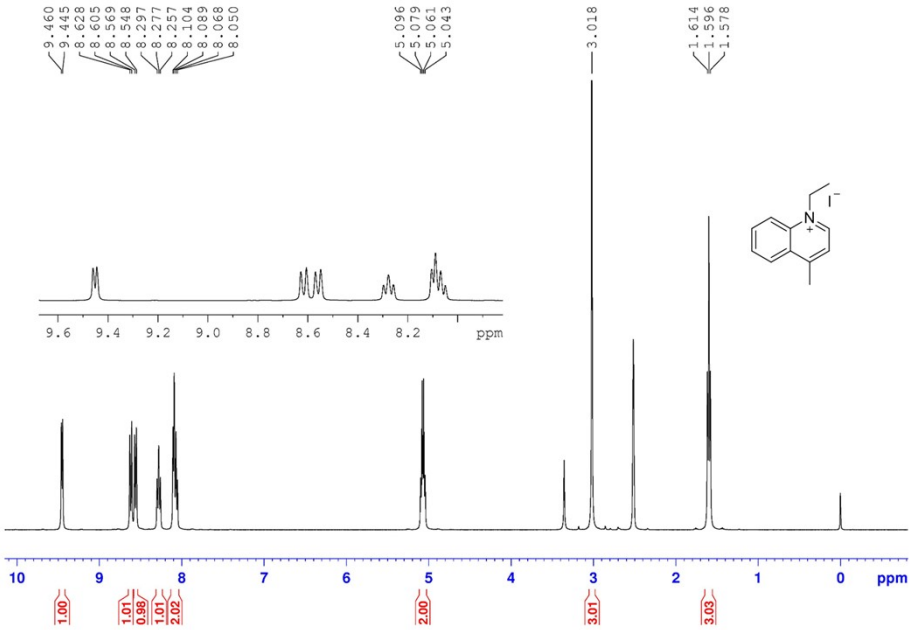

Fig. S12 ^{1}H NMR spectrum of **QM-Eth** in DMSO-d_6

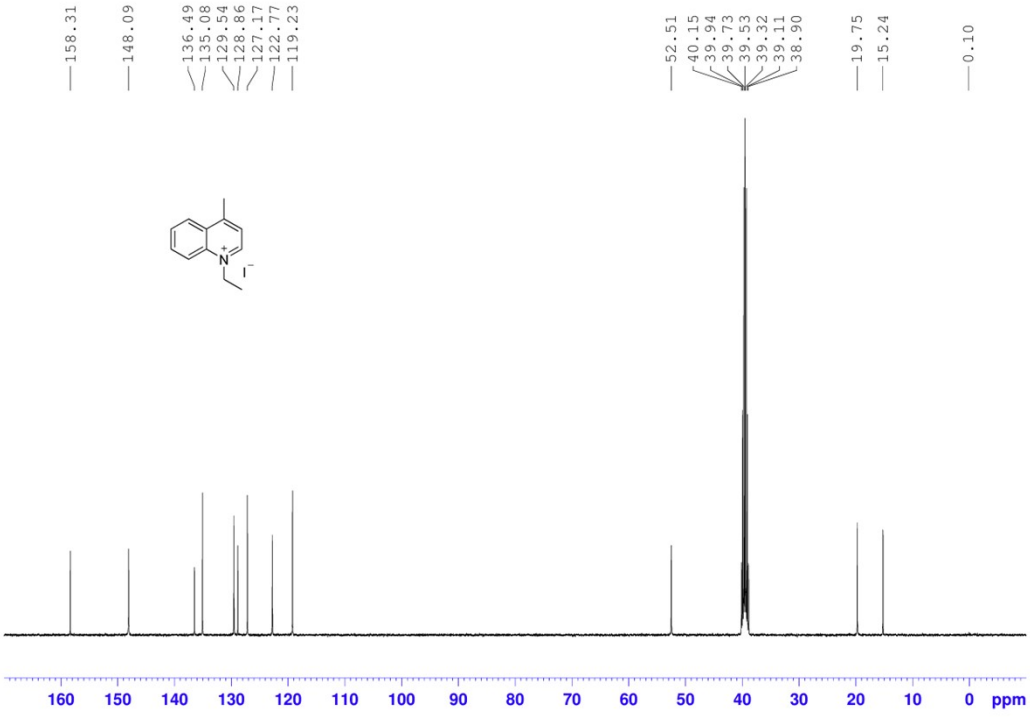

Fig. S13 ^{13}C NMR spectrum of **QM-Eth** in DMSO-d_6

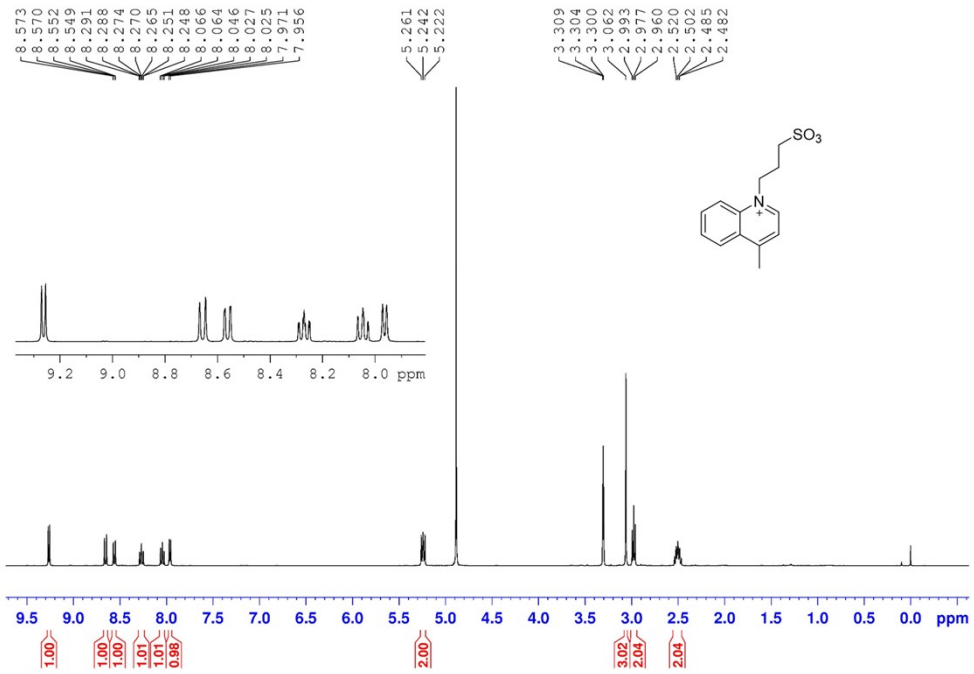

Fig. S14 [1]H NMR spectrum of **QM-PrS** in MeOD

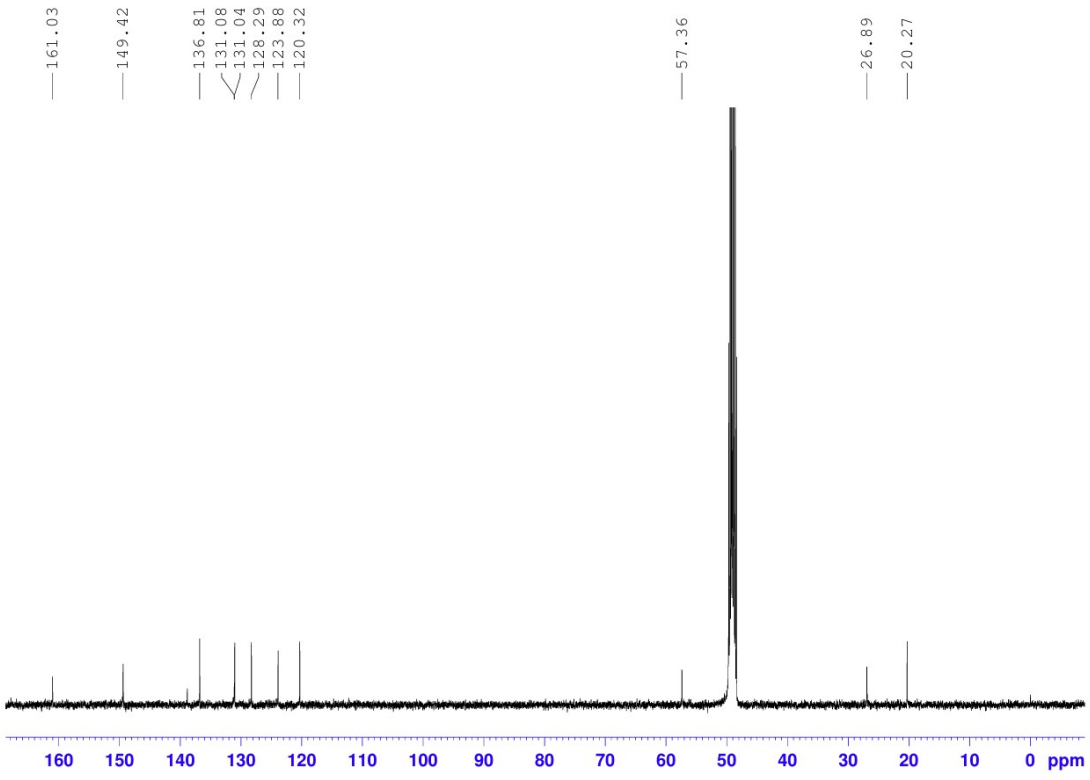

Fig. S15 [13]C NMR spectrum of **QM-PrS** in MeOD

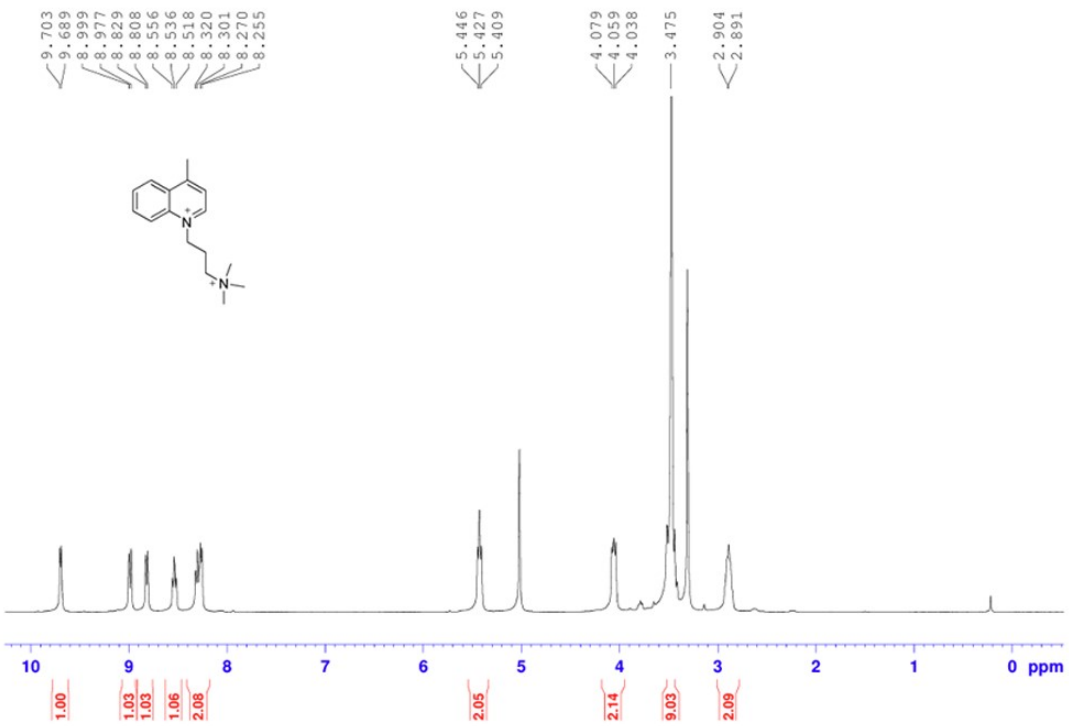

Fig. S16 ^{1}H NMR spectrum of **QM-PrN** in MeOD

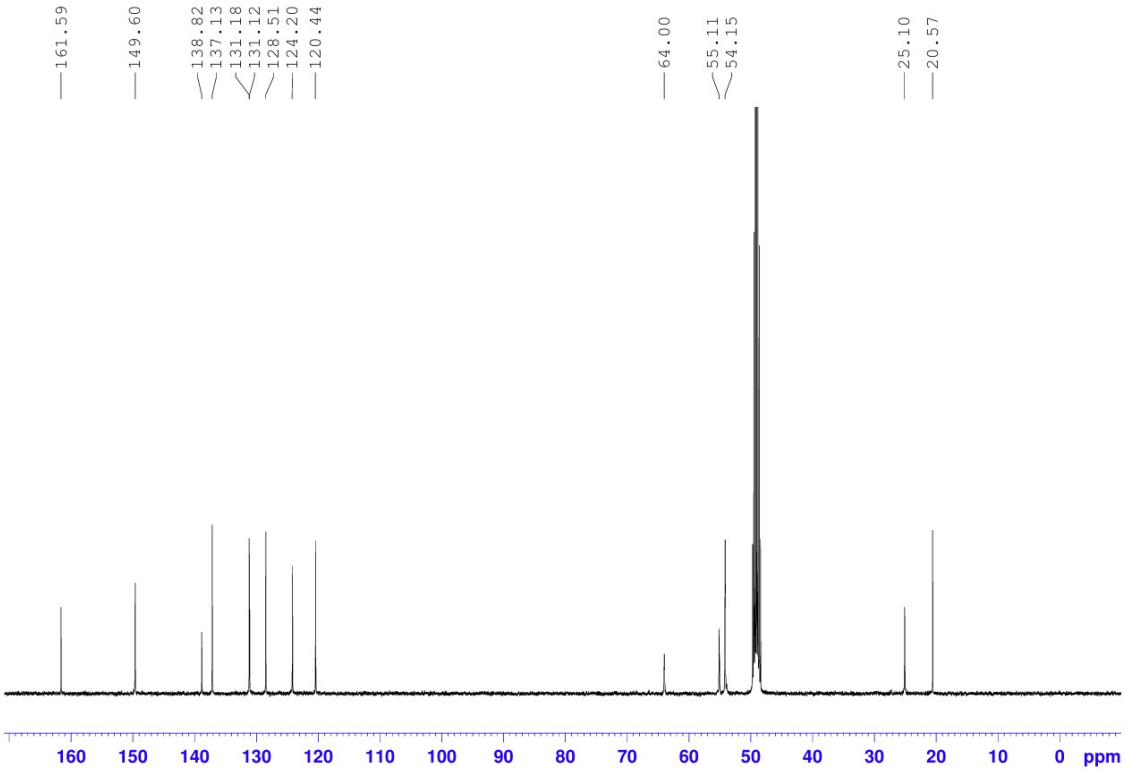

Fig. S17 ^{13}C NMR spectrum of **QM-PrN** in MeOD

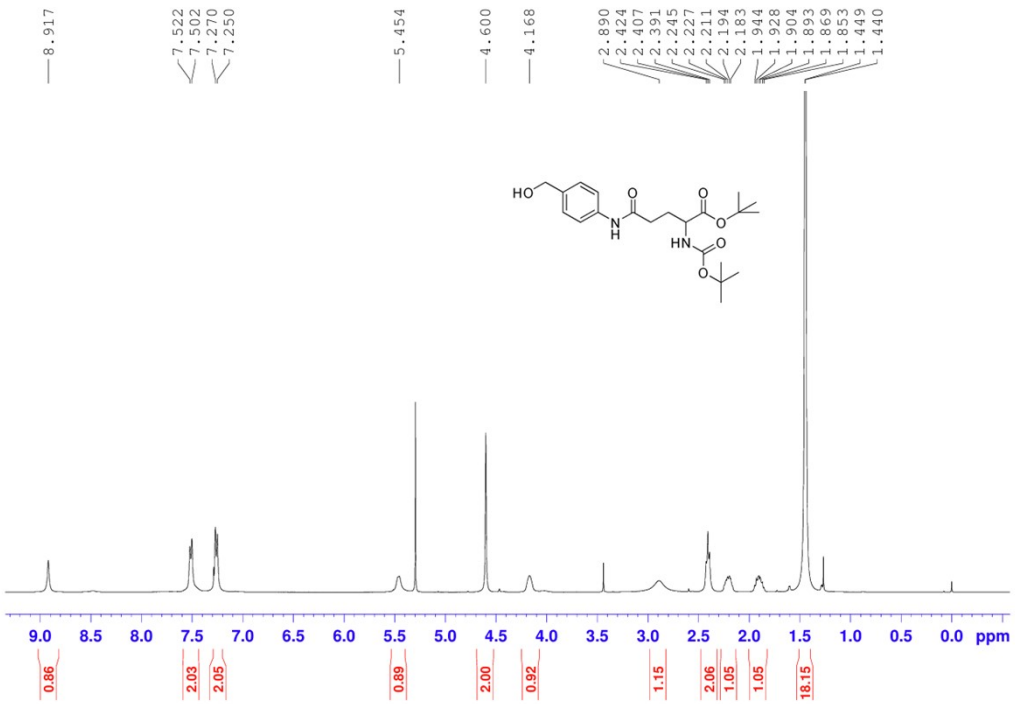

Fig. S18 ^{1}H NMR spectrum of **PAB-Glu-Boc** in $CDCl_3$

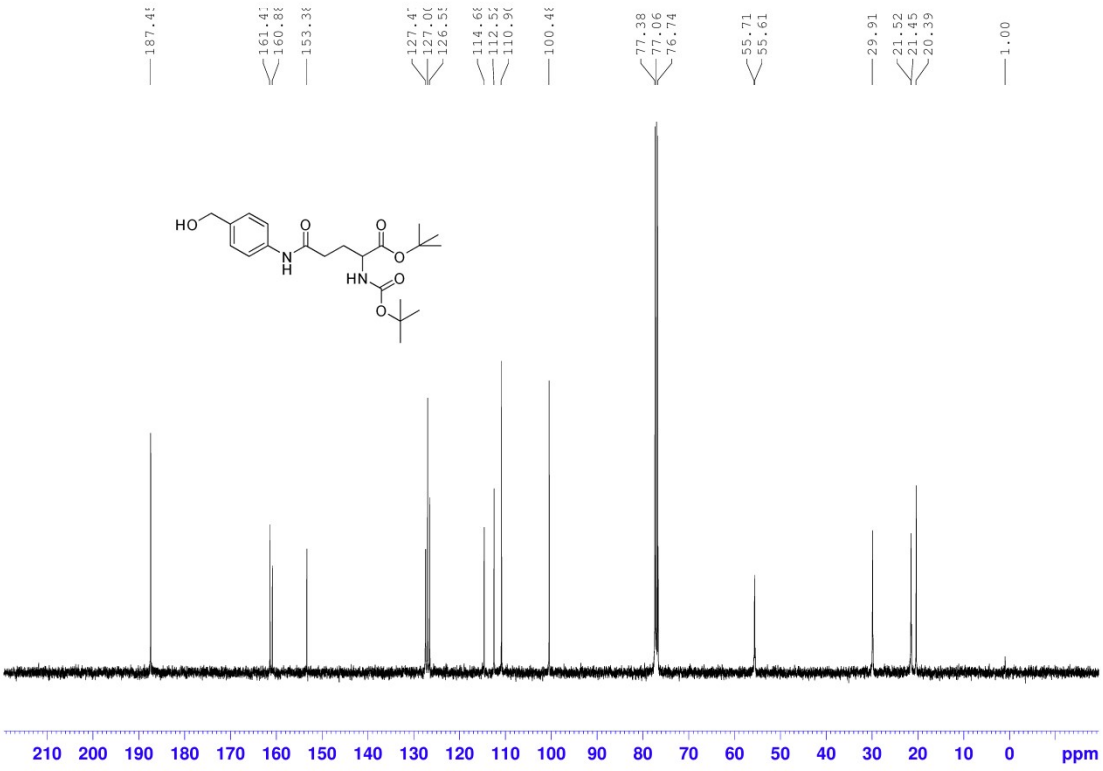

Fig. S19 ^{13}C NMR spectrum of **PAB-Glu-Boc** in $CDCl_3$

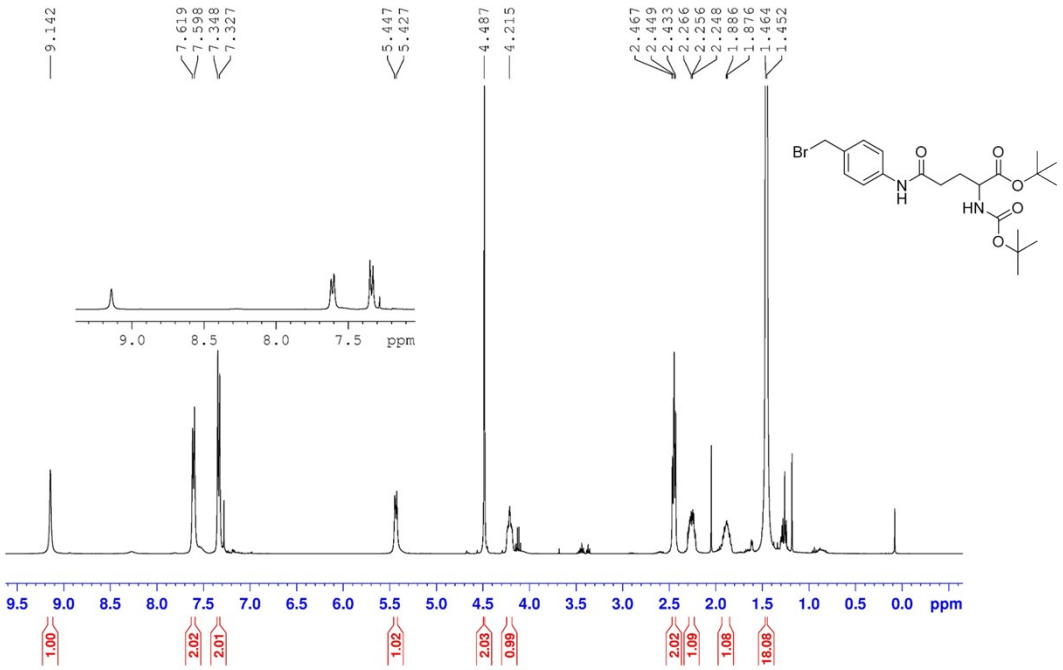

Fig. S20 ^{1}H NMR spectrum of **Br-Glu-Boc** in $CDCl_3$

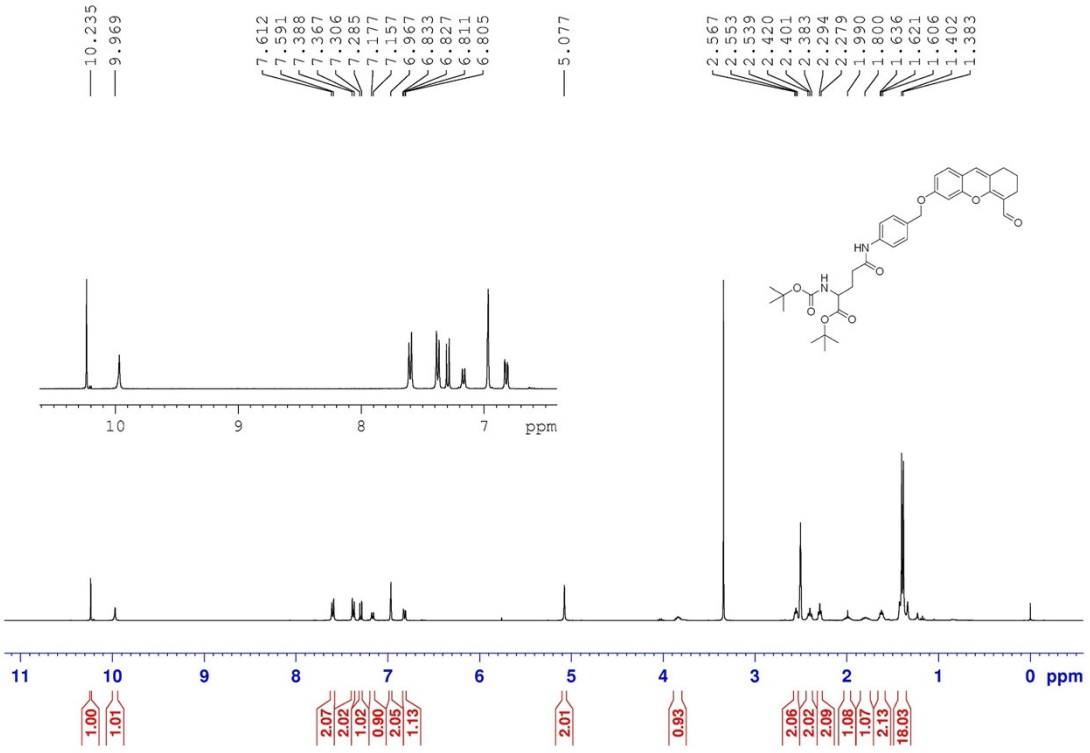

Fig. S21 ^{1}H NMR spectrum of **Glu-Boc-DDAO** in $CDCl_3$

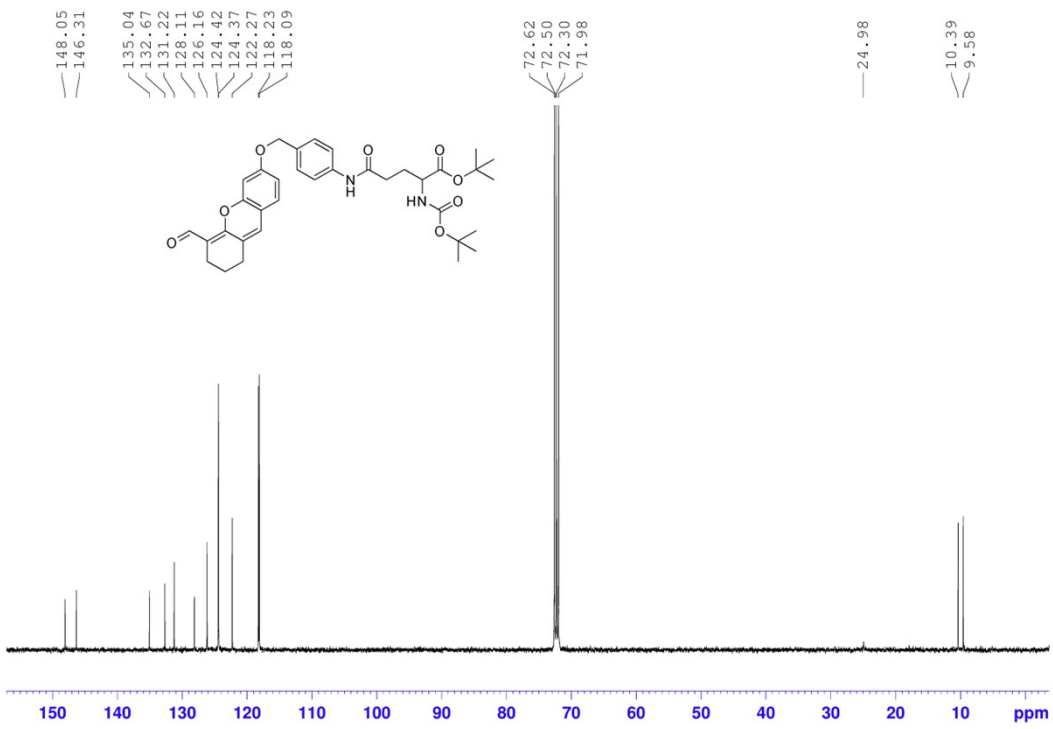

Fig. S22 ^{13}C NMR spectrum of **Glu-Boc-DDAO** in $CDCl_3$

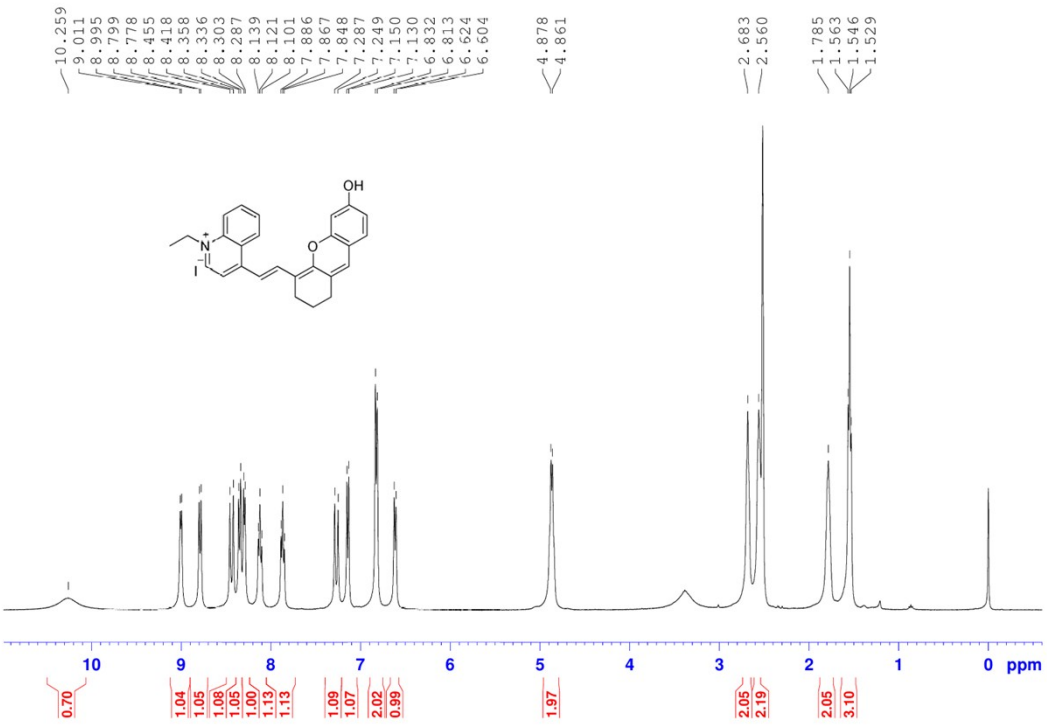

Fig. S23 ^{1}H NMR spectrum of **QMC-OH-C** in DMSO-d_6

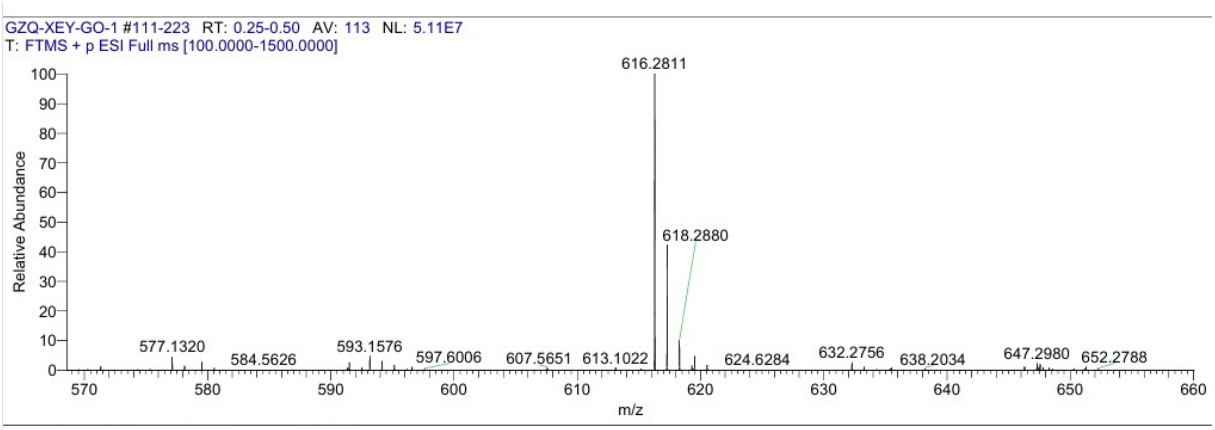

GZQ-XEY-GO-1#139 RT: 0.31
T: FTMS + p ESI Full ms [100.0000-1500.0000]
m/z= 616.22-616.69

m/z	Intensity	Relative	Theo. Mass	Delta (ppm)	Composition
616.2811	70401776.0	100.00	616.2806	0.47	$C_{38}H_{38}O_5N_3$

Fig. S24 HRMS spectrum of **QMC-OH-C**

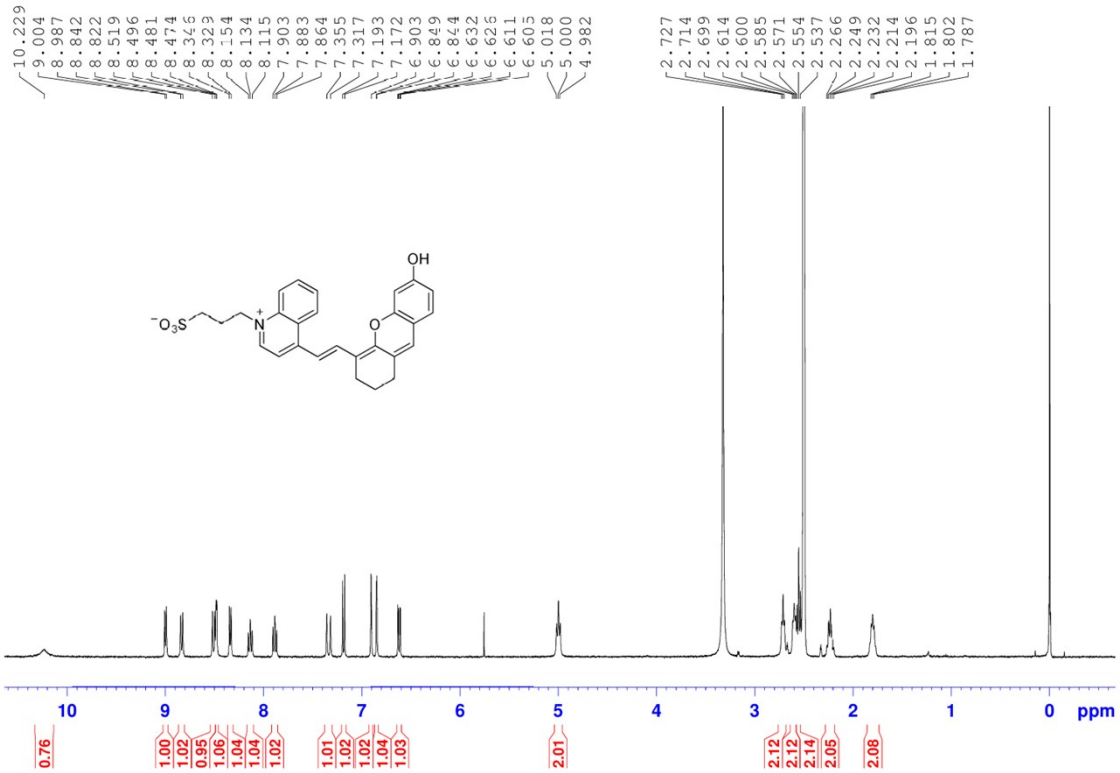

Fig. S25 ^{1}H NMR spectrum of QMC-OH-SO_3 in DMSO-d_6

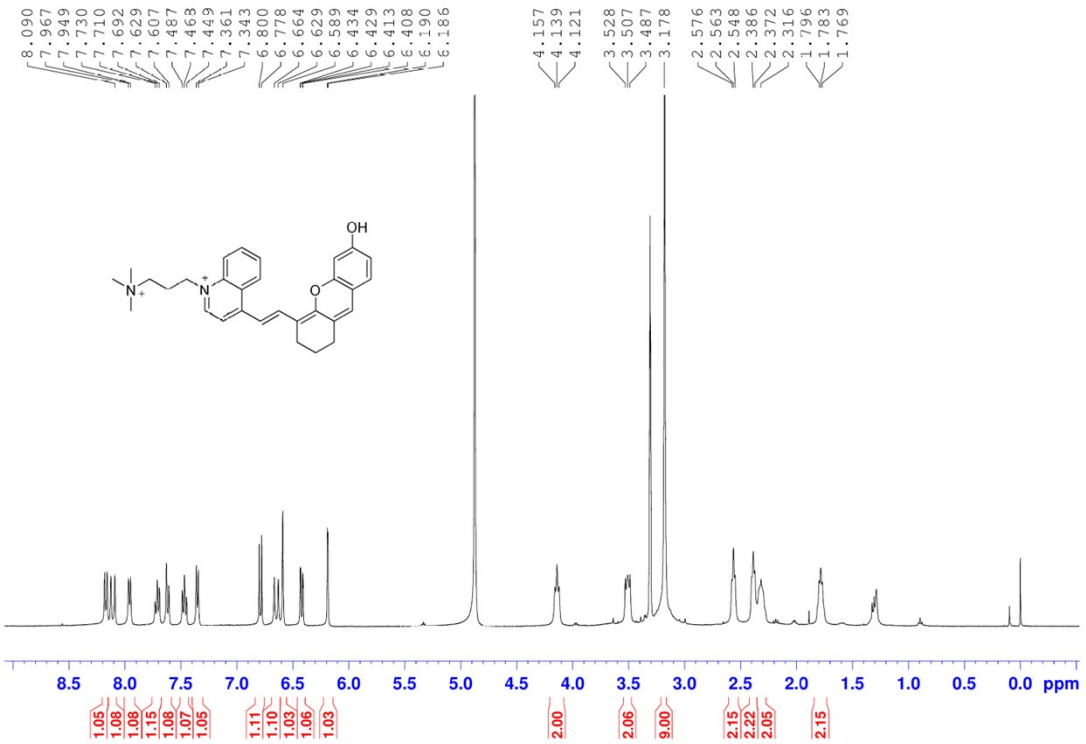

Fig. S26 ^{1}H NMR spectrum of QMC-OH-N in DMSO-d_6

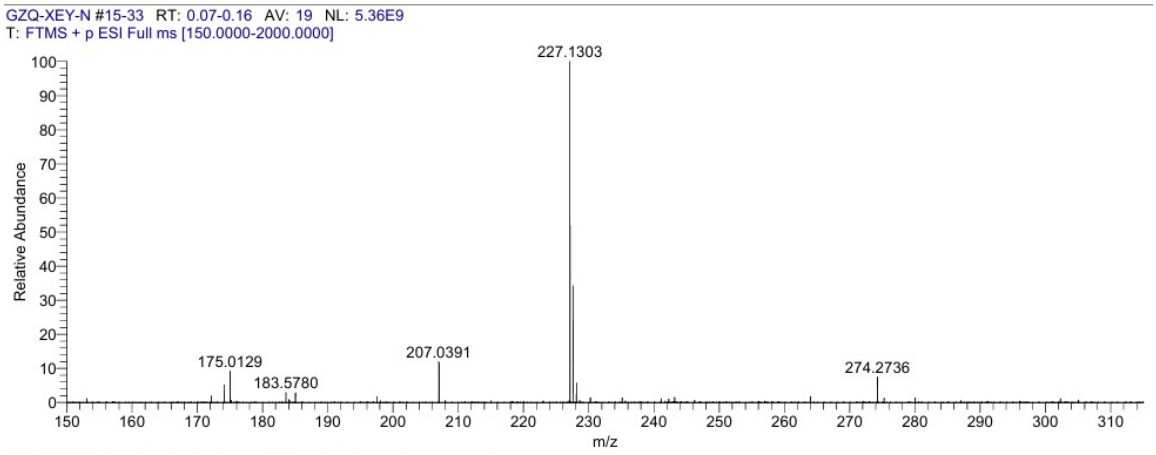

GZQ-XEY-N#15-33 RT: 0.07-0.16 AV: 19
T: FTMS + p ESI Full ms [150.0000-2000.0000]
m/z= 225.21-229.87

m/z	Intensity	Relative	Theo. Mass	Delta (ppm)	Composition
227.1303	5487167488.0	100.00	227.1305	-0.17	$C_{30}H_{34}O_2N_2$

Fig. S27 HRMS spectrum of QMC-OH-N

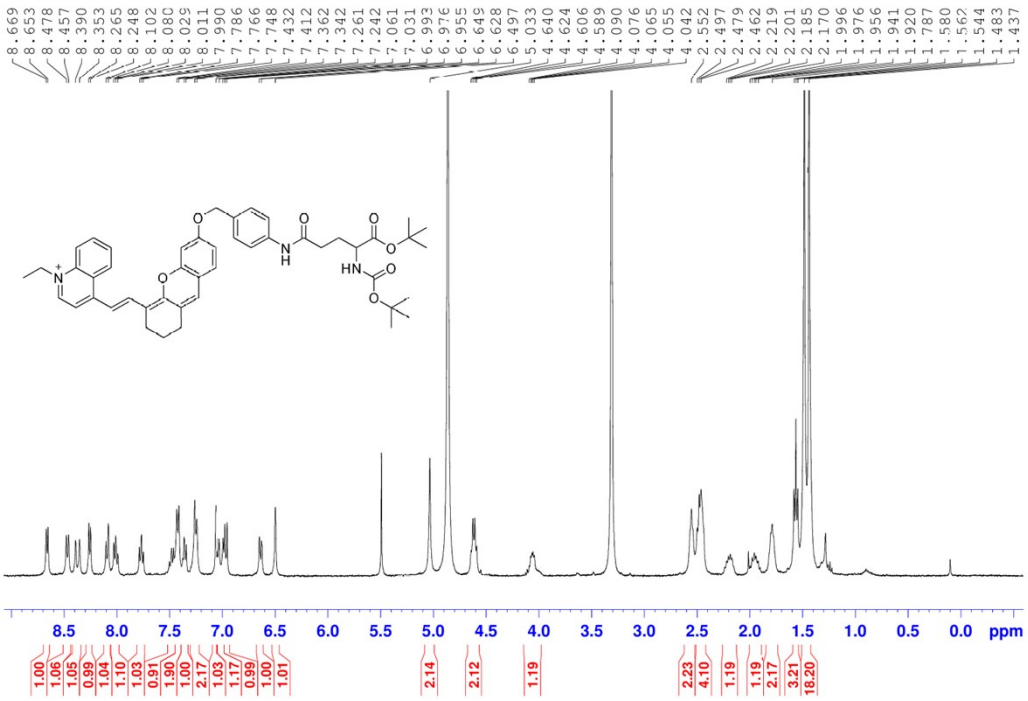

Fig. S28 ^{1}H NMR spectrum of QM-C-GGT-Boc in MeOD

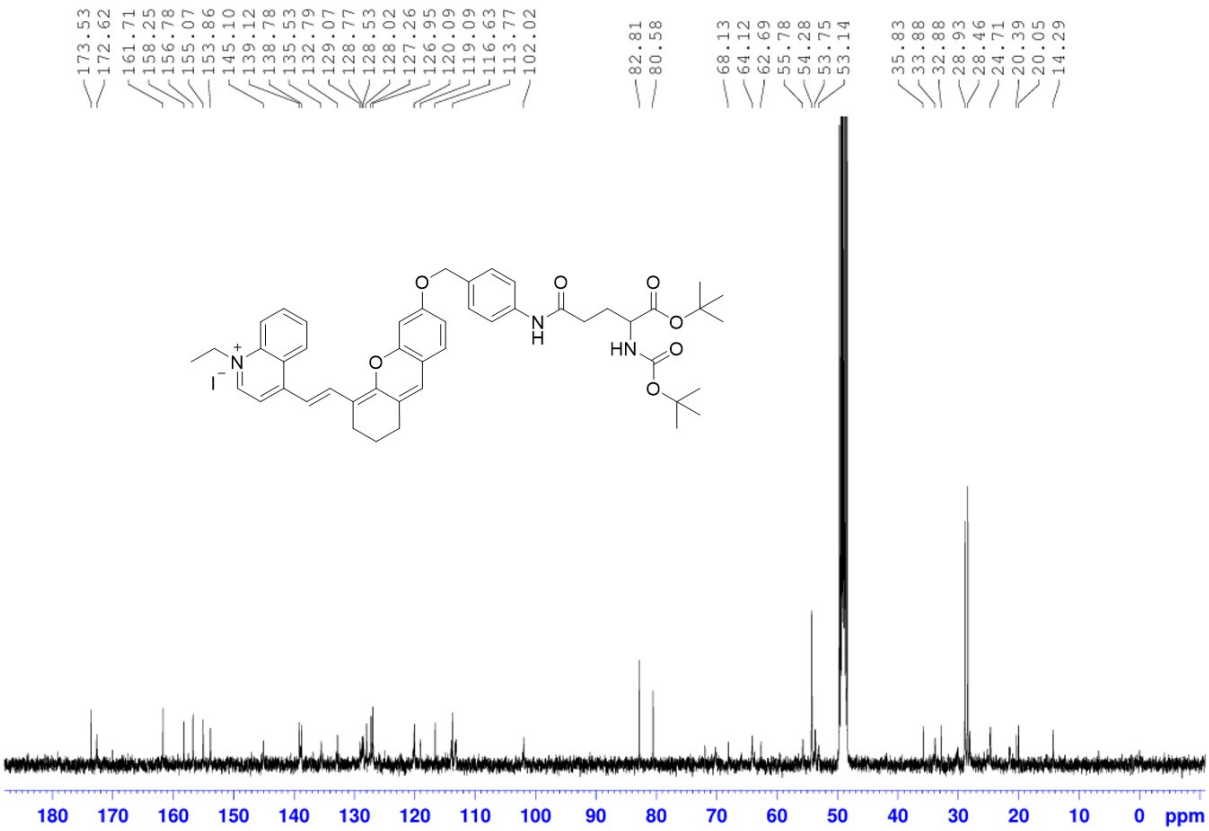

Fig. S29 ^{13}C NMR spectrum of QM-C-GGT-Boc in MeOD

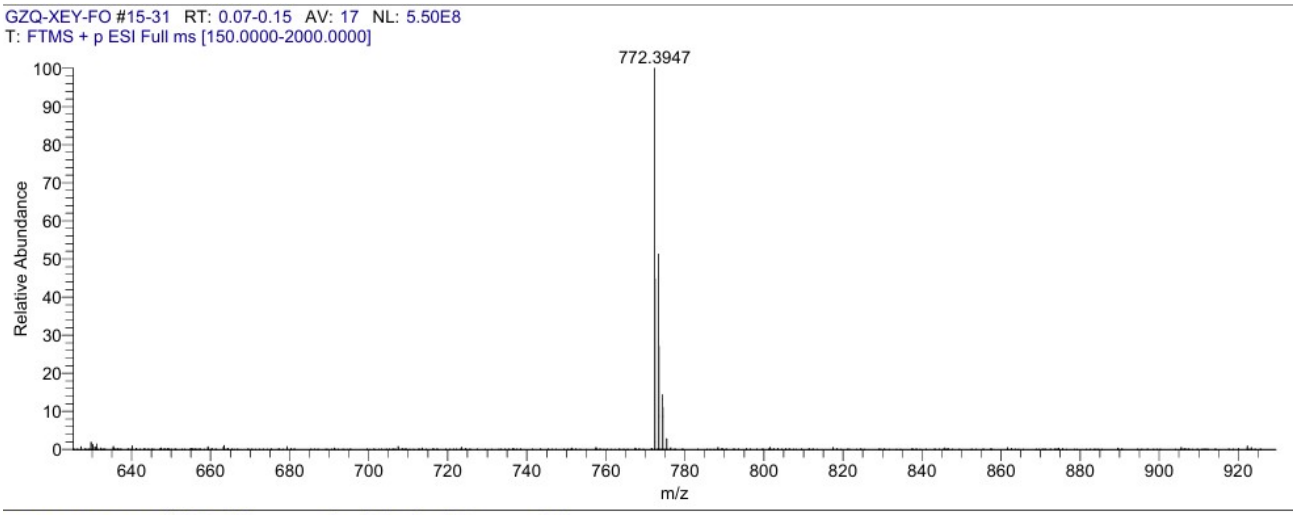

GZQ-XEY-FO#15-31 RT: 0.07-0.15 AV: 17
T: FTMS + p ESI Full ms [150.0000-2000.0000]
m/z= 769.28-777.86

m/z	Intensity	Relative	Theo. Mass	Delta (ppm)	Composition
772.3947	550267584.0	100.00	772.3956	-0.89	$C_{47}H_{54}O_7N_3$

Fig. S30 HRMS spectrum of QM-C-GGT-Boc

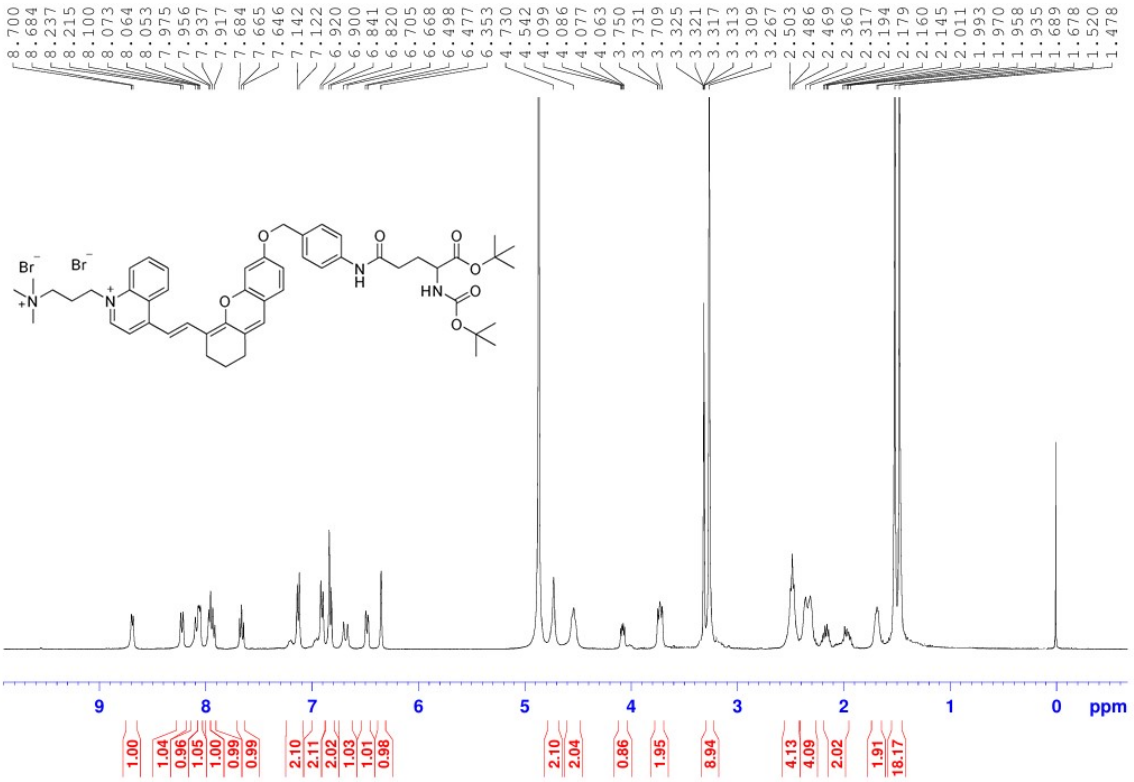

Fig. S31 ^{1}H NMR spectrum of QM-N-GGT-Boc in CD_3OD

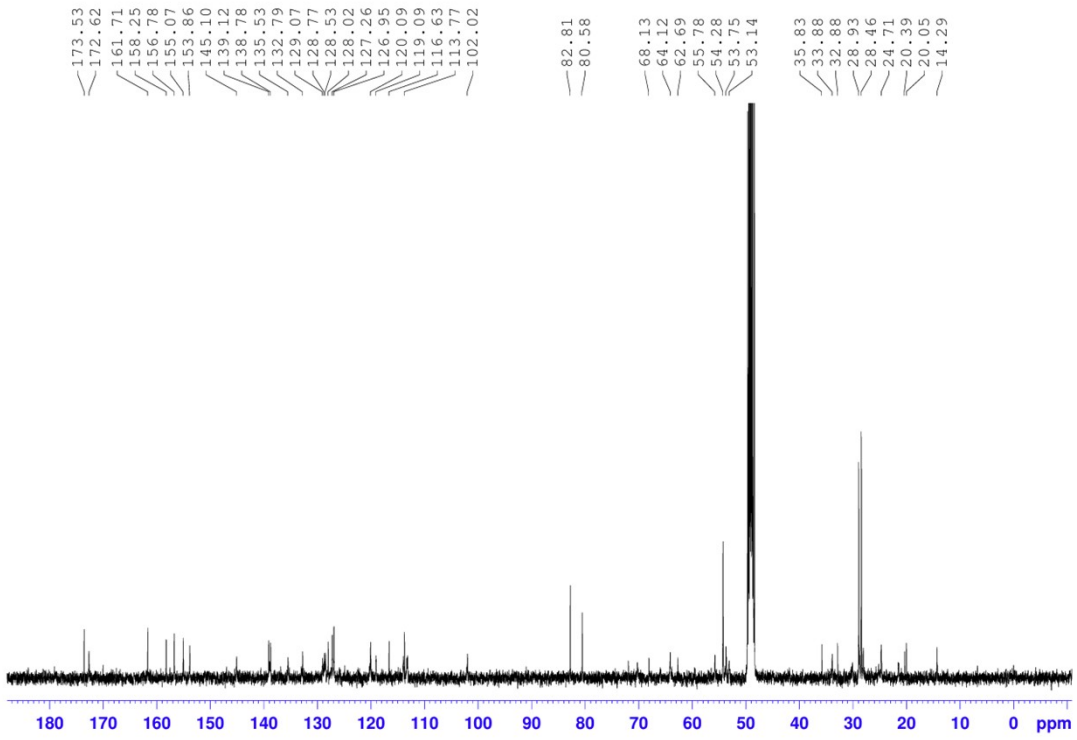

Fig. S32 ^{13}C NMR spectrum of QM-N-GGT-Boc in CD_3OD

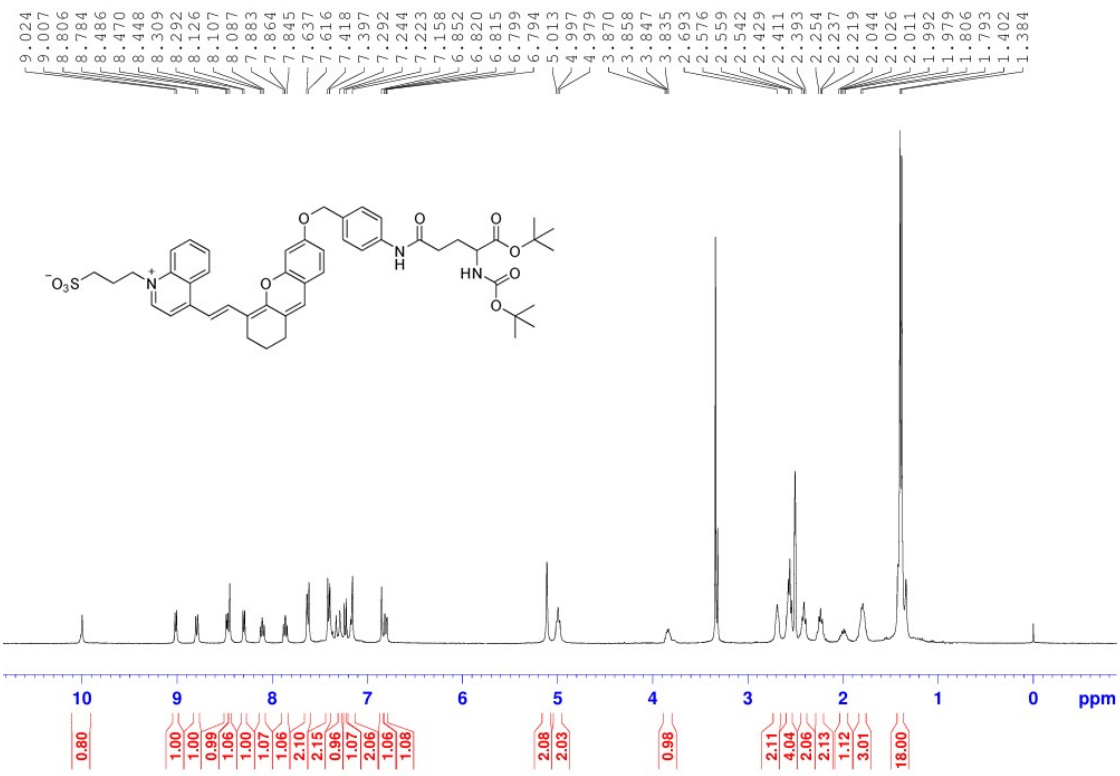

Fig. S33 ^{1}H NMR spectrum of QM-SO_3-GGT-Boc in DMSO-d_6

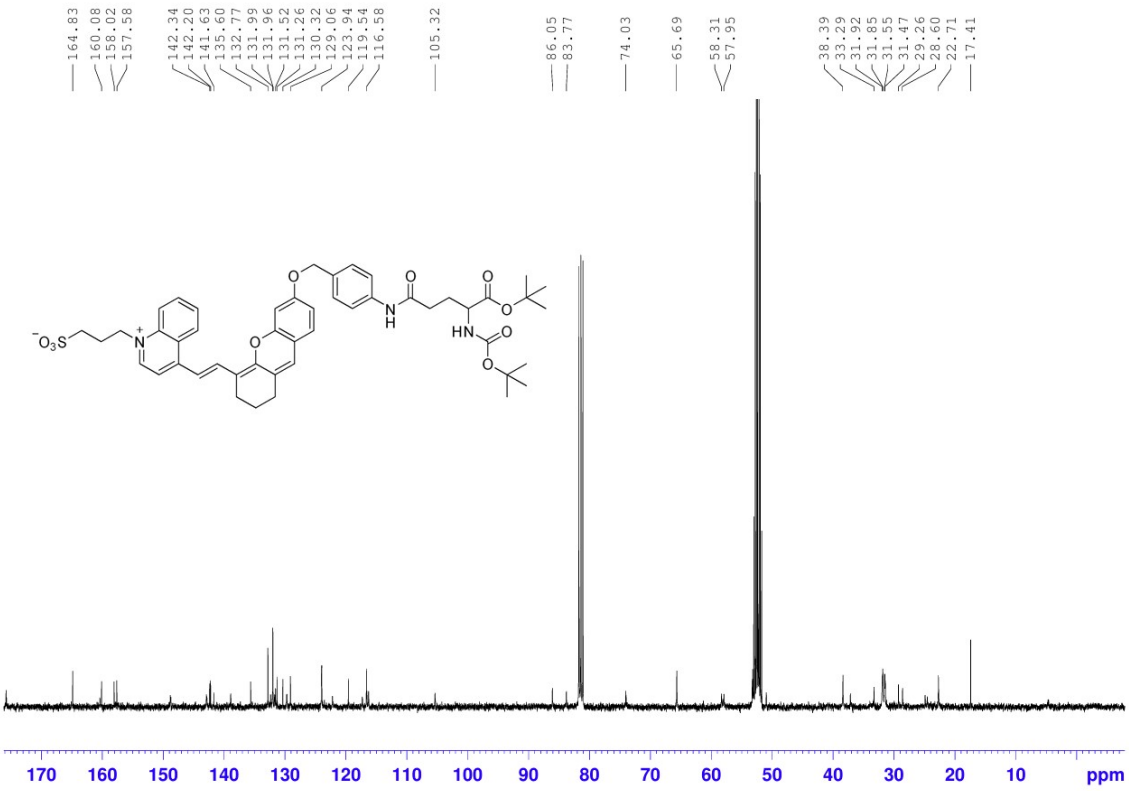

Fig. S34 ^{13}C NMR spectrum of QM-SO_3-GGT-Boc in DMSO-d_6

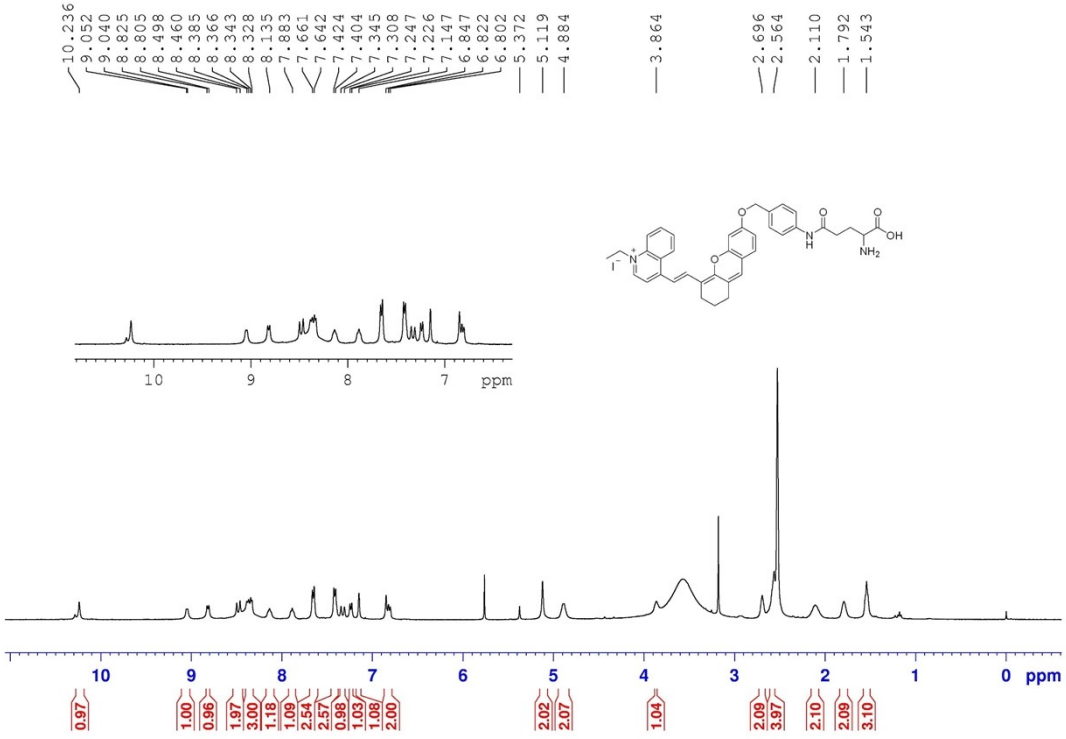

Fig. S35 ^{1}H NMR spectrum of QMC-C-GGT in DMSO-d_6

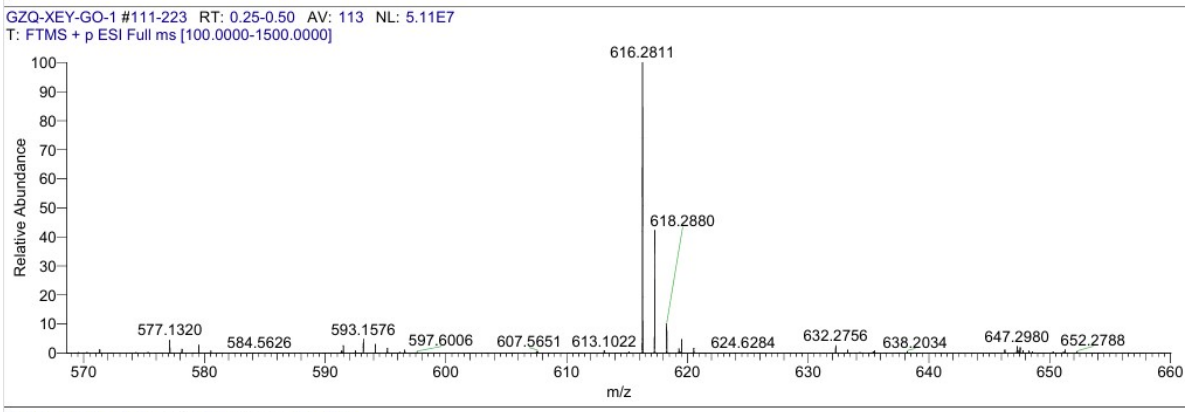

GZQ-XEY-GO-1#139 RT: 0.31
T: FTMS + p ESI Full ms [100.0000-1500.0000]
m/z= 616.22-616.69

m/z	Intensity	Relative	Theo. Mass	Delta (ppm)	Composition
616.2811	70401776.0	100.00	616.2806	0.47	$C_{38}H_{38}O_5N_3$

Fig. S36 HRMS spectrum of QMC-C-GGT

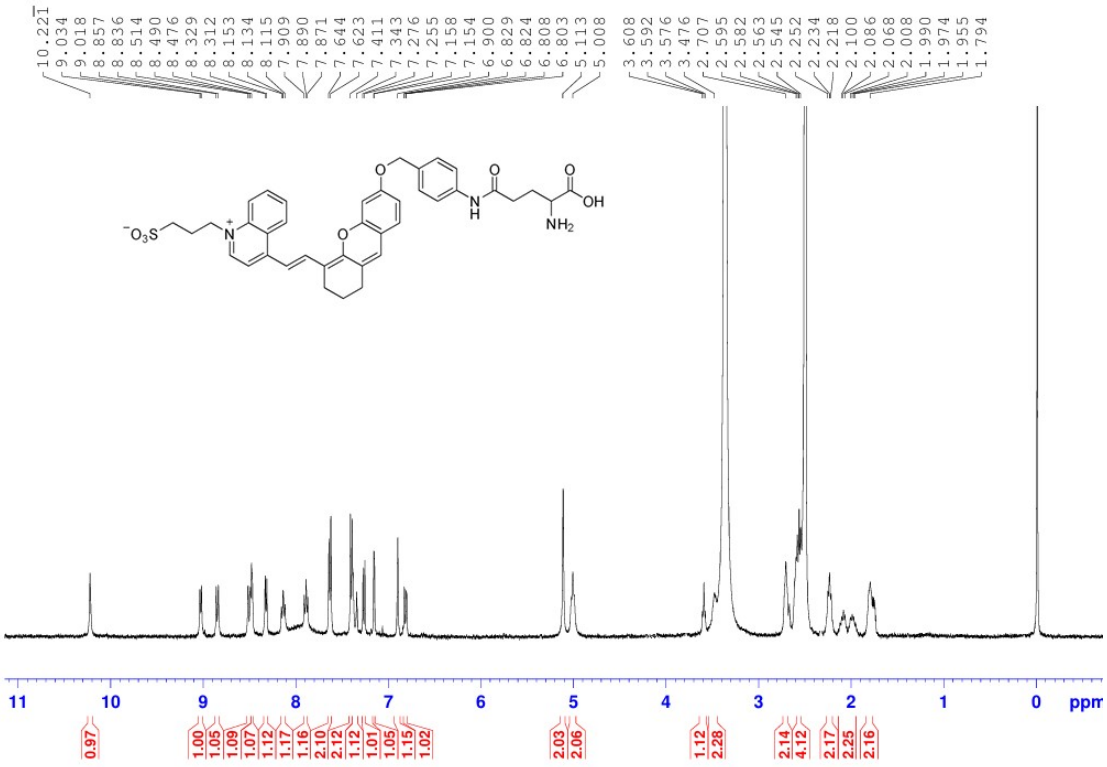

Fig. S37 ^{1}H NMR spectrum of QMC-SO_3-GGT in DMSO-d_6

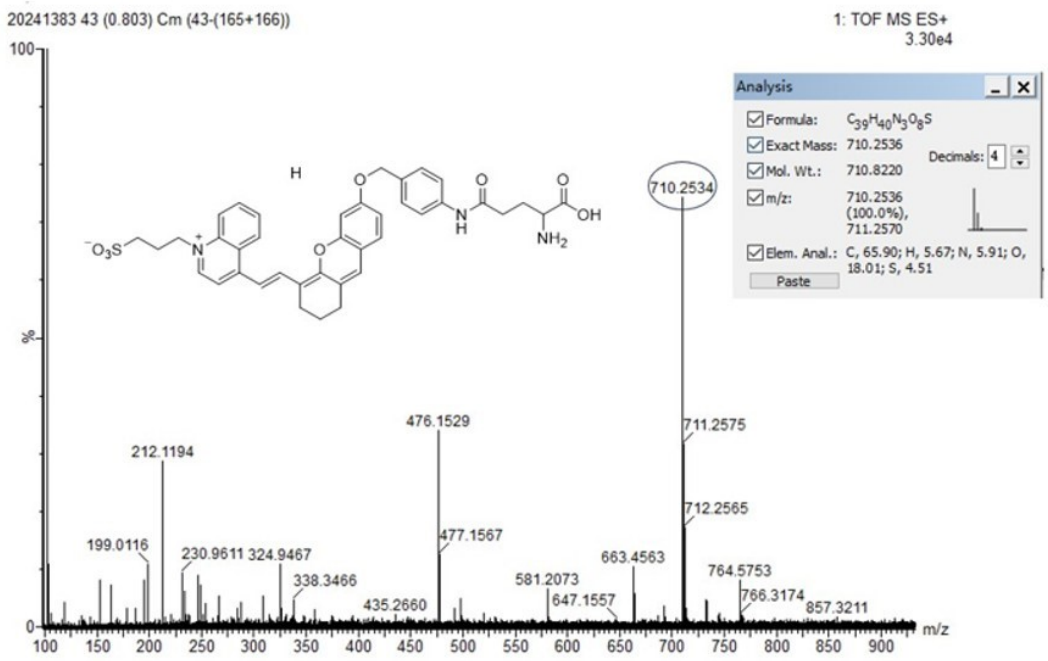

Fig. S38 HRMS spectrum of QMC-SO_3-GGT

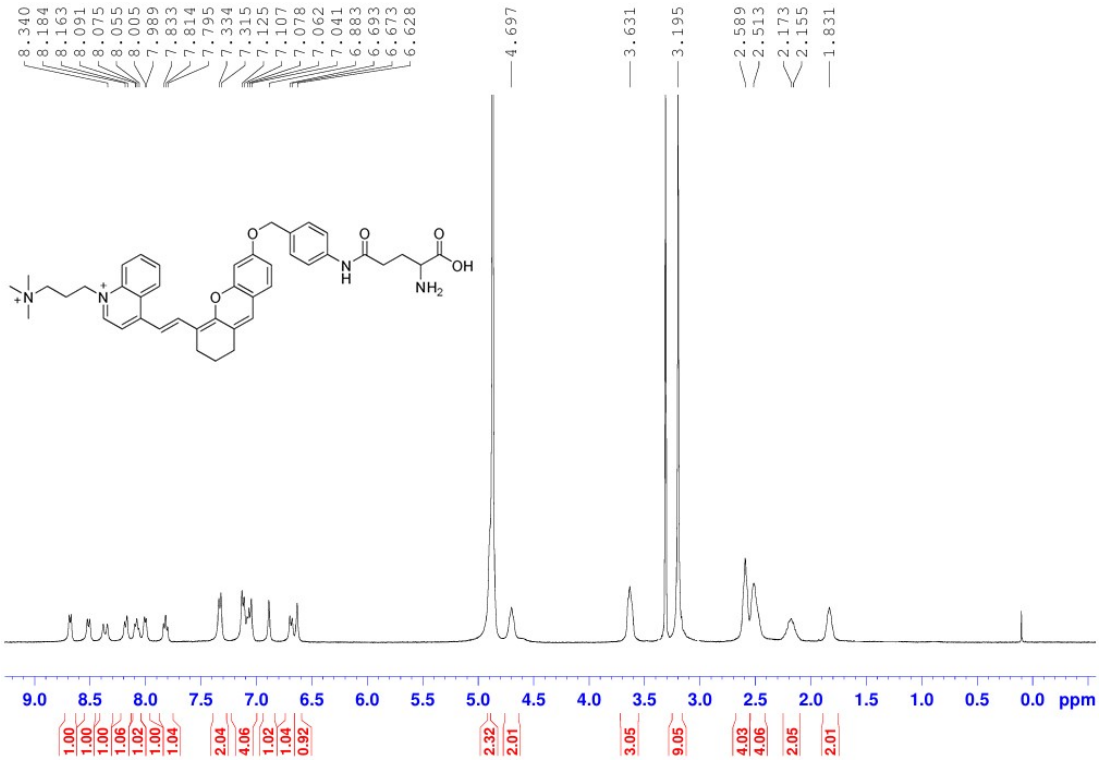

Fig. S39 ^{1}H NMR spectrum of QMC-N-GGT in MeOD

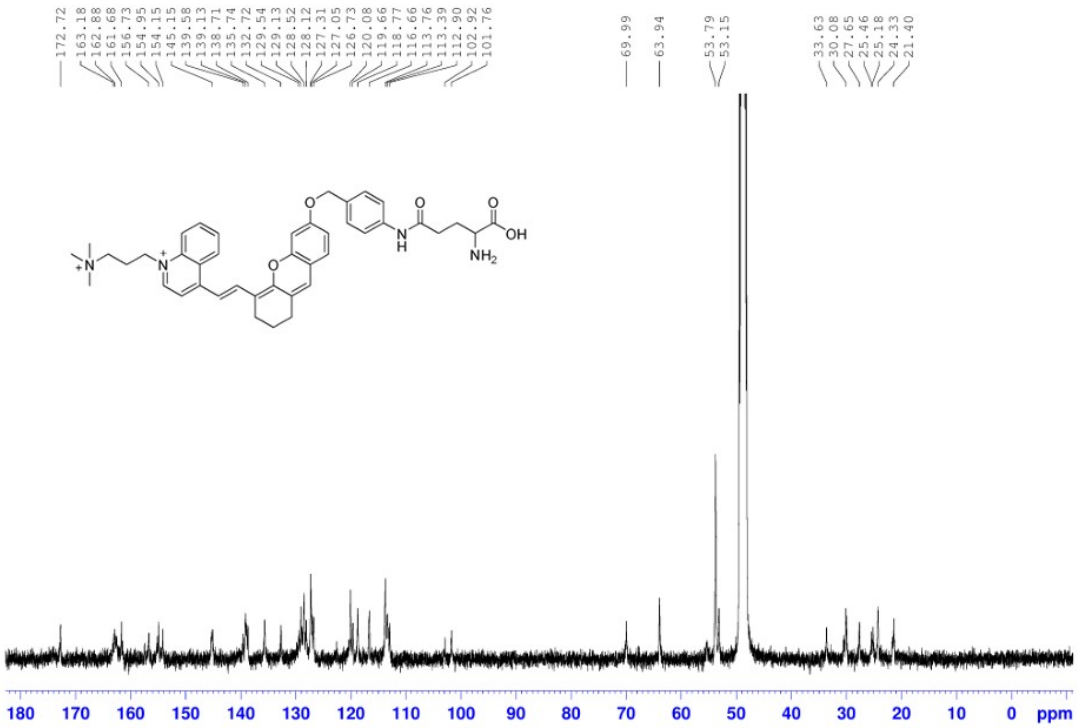

Fig. S40 ^{13}C NMR spectrum of QMC-N-GGT in MeOD

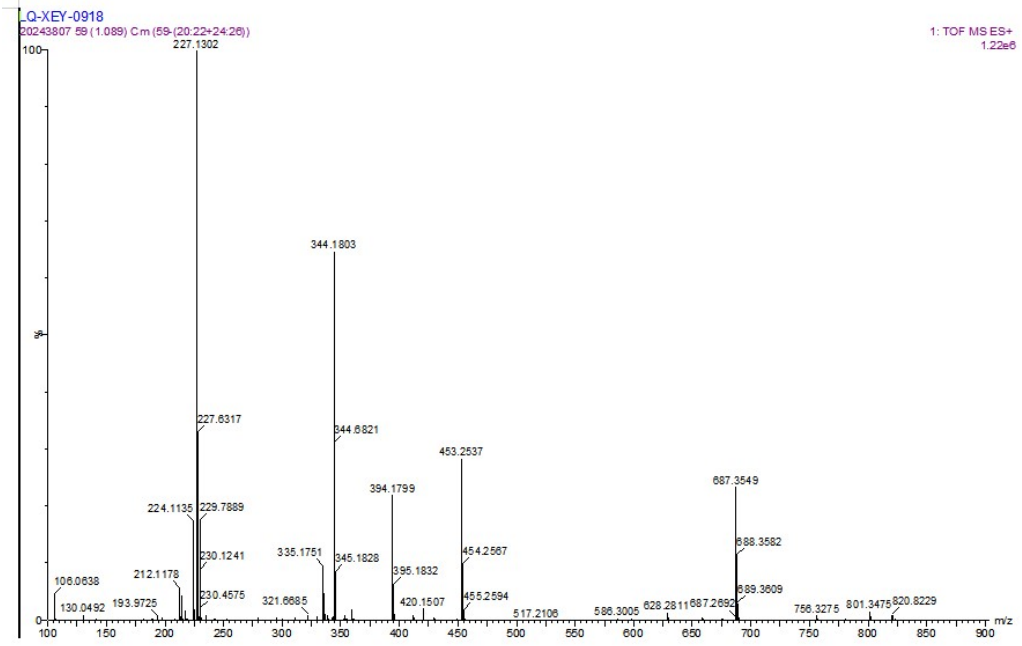

Fig. S41 HRMS spectrum of QMC-N-GGT